Molecular Characterization of the 50-kD Subunit of Dynactin Reveals Function for the Complex in Chromosome Alignment and Spindle Organization during Mitosis

Christophe J. Echeverri,*‡ Bryce M. Paschal,§ Kevin T. Vaughan,* and Richard B. Vallee*

*Cell Biology Group, Worcester Foundation for Biomedical Research, Shrewsbury, Massachusetts 01545;‡Department of Cell Biology, University of Massachusetts Graduate School of Biomedical Sciences, Worcester, Massachusetts 01655; and §Department of Cell Biology, The Scripps Research Institute, La Jolla, California 92037

Abstract. Dynactin is a multi-subunit complex which has been implicated in cytoplasmic dynein function, though its mechanism of action is unknown. In this study, we have characterized the 50-kD subunit of dynactin, and analyzed the effects of its overexpression on mitosis in living cells. Rat and human cDNA clones revealed p50 to be novel and highly conserved, containing three predicted coiled-coil domains. Immunofluorescence staining of dynactin and cytoplasmic dynein components in cultured vertebrate cells showed that both complexes are recruited to kinetochores during prometaphase, and concentrate near spindle poles thereafter. Overexpression of p50 in COS-7 cells disrupted mitosis, causing cells to accumulate in a prometaphase-like state. Chromosomes were condensed but unaligned, and spindles, while still bipolar, were dramatically distorted. Sedimentation analysis revealed the dynactin complex to be dissociated in the transfected cultures. Furthermore, both dynactin and cytoplasmic dynein staining at prometaphase kinetochores was markedly diminished in cells expressing high levels of p50. These findings represent clear evidence for dynactin and cytoplasmic dynein codistribution within cells, and for the presence of dynactin at kinetochores. The data also provide direct in vivo evidence for a role for vertebrate dynactin in modulating cytoplasmic dynein binding to an organelle, and implicate both dynactin and dynein in chromosome alignment and spindle organization.

Cytoplasmic dynein is a ubiquitous, multi-subunit ATPase responsible for minus end–directed microtubule-based organelle transport (Paschal and Vallee, 1987; Holzbaur and Vallee, 1994). It is thought to be responsible for retrograde axonal transport (Paschal and Vallee, 1987; Schnapp and Reese, 1989; Schroer et al., 1989; Lacey and Haimo, 1992) and the perinuclear distribution of a number of organelles, including the Golgi apparatus (Corthésy-Theulaz et al., 1992; Fath et al., 1994), late endosomes, and lysosomes (Lin and Collins, 1992; Aniento et al., 1993). Several lines of evidence have also implicated cytoplasmic dynein in mitosis, though its precise role has remained uncertain. The motor has been localized in some studies to the prometaphase kinetochore of vertebrate chromosomes (Pfarr et al., 1990; Steuer et al., 1990; but see Lin and Collins, 1992). Consistent with this result, rapid minus end–directed chromosome movements have been observed in cells during early prometaphase (Rieder and Alexander, 1990; for review see Rieder and Salmon, 1994). Kinetochores of isolated chromosomes have also been reported to exhibit retrograde motor activity (Hyman and Mitchison, 1991). Although these findings suggest a role in chromosome movement, microinjection of anti-cytoplasmic dynein antibodies (Vaisberg et al., 1993) has been found to result instead in spindle collapse, apparently implicating the motor in some aspect of spindle organization. Phenotypic analysis of yeast cytoplasmic dynein disruption strains has indicated a role in spindle positioning (Eshel et al., 1993; Li et al., 1993) and some participation in anaphase chromosome segregation (Saunders et al., 1995). These functions seem to be manifestations of a more general role in nuclear positioning and migration in yeast (Eshel et al., 1993; Li et al., 1993) and other fungi (Plamann et al., 1994; Xiang et al., 1994).

In addition to uncertainties over the full range of cytoplasmic dynein functions, little is understood about the regulation of its activity and the mechanism by which it is targeted to a specific subset of intracellular organelles. One reported regulatory factor is dynactin, which was identified as a fraction that could be separated out of sucrose gradient-purified cytoplasmic dynein preparations, and which stimulated the frequency of minus-end directed

Address all correspondence to Dr. Richard Vallee, Worcester Foundation for Biomedical Research, 222 Maple Avenue, Shrewsbury, MA 01545. Tel.: 508-842-8921. Fax: 508-842-3915. e-mail: vallee@sci.wfbr.edu

particle movements in an in vitro assay (Gill et al., 1991; Schroer and Sheetz, 1991). Components of this fraction could also be coimmunoprecipitated out of brain cytosol (Paschal et al., 1993), and appear as a discrete particle by electron microscopy (Schafer et al., 1994). Purified dynactin contains at least nine polypeptides ranging from 24 to 150 kD (Gill et al., 1991; Paschal et al., 1993; Schafer et al., 1994). It consists of an F-actin–like core filament composed of the actin-related protein Arp1 (Clark and Meyer, 1992; Lees-Miller et al., 1992; Paschal et al., 1993), with a capping protein heterodimer bound at one extremity, and a 62-kD component at the other (Schafer et al., 1994). Extending laterally from the filament is the largest subunit of the complex, p150^{Glued} (Schafer et al., 1994). This polypeptide has been found to be homologous throughout its length to the product of the *Glued* gene in *Drosophila* (Holzbaur et al., 1991; Gill et al., 1991), which is involved in neuronal development and possibly other more general cellular functions (Harte and Kankel, 1982).

The specific role of dynactin in modulating cytoplasmic dynein function is unknown. Although the two complexes partially copurify through the microtubule sedimentation and ATP extraction steps of the cytoplasmic dynein preparative procedure (Collins and Vallee, 1989; Gill et al., 1991, Paschal et al., 1993), they show limited evidence of an interaction after extraction from microtubules, or when either is immunoprecipitated directly from cytosolic extracts (Paschal et al., 1993). Nonetheless, recent evidence has revealed direct binding between recombinant cytoplasmic dynein intermediate chains (IC)[1] and p150^{Glued} (Vaughan and Vallee, 1995; Karki and Holzbaur, 1995). These data indicate that the two complexes can interact directly and suggest that the interaction between the complete complexes must be regulated. An interaction between dynein and dynactin in cells has been difficult to test by immunocytochemical means. This is in part due to the high density of fine punctate staining observed for dynactin in interphase cells (Gill et al., 1991; Clark and Meyer, 1992; Paschal et al., 1993). Furthermore, during mitosis, dynactin was not observed to associate with kinetochores (Gill et al., 1991). Nevertheless, homologues of Arp1 and p150^{Glued} have been deduced to function in a common pathway with cytoplasmic dynein based on phenotypic similarities and suppressor analysis in *S. cerevisiae* (Muhua et al., 1994; Clark and Meyer, 1994), *Neurospora* (Plamann et al., 1994), and *Drosophila* (McGrail et al., 1995).

The present study was initiated to gain further insight into the function of dynactin and its relationship to cytoplasmic dynein. We have cloned p50, the second most abundant component of dynactin (4–5 moles per mole of complex; Paschal et al., 1993; Schafer et al., 1994) and analyzed its distribution and the effects of its overexpression in cultured mammalian cells. We report that dynactin, like cytoplasmic dynein, is recruited to prometaphase kinetochores, and present direct in vivo evidence for a specific role for vertebrate dynactin in prometaphase chromosome alignment and spindle organization during higher eukaryotic mitosis.

1. *Abbreviations used in this paper*: CREST, calcinosis, Raynaud's phenomenon, esophageal dysmotility, sclerodactyly, telangiectasia; EST, expressed sequence tag; HTH, helix-turn-helix; IC, intermediate chain; NEB, nuclear envelope breakdown.

Materials and Methods

Peptide Sequencing

The dynactin complex was immunoprecipitated out of calf brain cytosol as previously described (Paschal et al., 1993), separated by SDS-PAGE (9% minigel, BioRad Laboratories, Richmond, CA), and electrophoretically transferred to nitrocellulose (Schleicher and Schuell, Keene, NH). After Ponceau S staining and destaining, the p50 band was excised, subjected to in situ trypsin digestion, and the eluted peptides were separated by C_{18} reverse-phase HPLC as previously described (Aebersold, 1989). NH_2-terminal amino acid sequence from six peptides was determined on a 477A Sequenator (Applied Biosystems, Foster City, CA), with a 120A phenylthiohydantoin analyzer by Dr. J. Leszyk of the Worcester Foundation for Biomedical Research Protein Chemistry Facility (Shrewsbury, MA).

Cloning of p50

The peptide No. 21 sequence was used to design an inosine-containing, partially degenerate oligonucleotide probe, composed of equal amounts of two oligonucleotides: (5′-AAT-GA[G,A]-CCI-GAT-GTI-TAT-GA[G,A]-ACI-AG[C,T]-GA[C,T]-TT[G,A]-CC[G,T,A]-GA-3′ and 5′-AAT-GA-[G,A]-CCI-GAT-GTI-TAT-GA[G,A]-ACI-TCI-GA[C,T]-CTI-CC[G,T,A]-GA-3′). This probe was [^{32}P] end-labeled, and used for hybridization screening of a bovine brain λgt10 cDNA library (No. BL1027a, Clontech Laboratories, Palo Alto, CA), in tetramethylammonium chloride (TMAC) solution (Jacobs et al., 1988) containing 3 M TMAC, 0.1 M $NaPO_4$ (pH 6.8), 1 mM EDTA (pH 8.0), 5× Denhardt's solution, 0.6% SDS, 100 μg/ml denatured salmon sperm DNA, at 53°C for 18 h. Filters were then washed in 3 M TMAC 50 mM Tris-HCl (pH 8.0), 0.2% SDS at room temperature for 15 min, followed by 53°C for 1 h. The TMAC was removed from the filters by three 10-min washes in 2× SSC, 0.1% SDS at room temperature. Bacteriophage from one positive plaque (B14A) were picked, purified by two more rounds of screening, and the insert DNA was sequenced (Sequenase version 2.0, US Biochemical, Cleveland, OH).

The B14A insert was EcoRI excised, labeled with α[^{32}P]dCTP by random priming (Boehringer Mannheim Biochemicals, Indianapolis, IN), and used for hybridization screening of a rat brain λZAPII cDNA library (No. 936515, Stratagene, La Jolla, CA). Hybridization was performed overnight at 65°C, in Rapid-Hyb solution (Amersham Corp., Arlington Heights, IL), and washes were according to the supplier's protocols, except that SSPE was used instead of SSC. The insert from one partial clone (R4A) was EcoRI excised and used to rescreen the same library as described above, yielding 12 positive clones. Two of these were found to be full-length (R11C, R11D).

A human expressed sequence tag cDNA clone (EST06385) (Adams et al., 1993), identified using the B14A insert sequence in a BLAST search (Altschul et al., 1990) of the National Center for Biotechnology Information (NCBI, Bethesda, MD) databases, was obtained from ATCC (renamed H50A), and fully sequenced. All DNA and protein sequence was assembled and analyzed using the GCG analysis programs, including MOTIFS and BESTFIT. The NCBI databases were also scanned using FASTA (Lipman and Pearson, 1988). The statistical significance of sequence alignments was determined using the RDF program (Lipman and Pearson, 1985), and additional homology was examined using the BLOCKS e-mail server (database version 7.01, Henikoff and Henikoff, 1994).

For bacterial expression of p50, the H50A coding region was subcloned into the pET-14b expression vector (Novagene, Madison, WI) after PCR mutagenesis and standard cloning techniques. After transformation into the *E. coli* expression strain *BL21(DE3)* and induction with 0.4 mM IPTG, bacteria were lysed in standard SDS-PAGE sample buffer, and analyzed by Western blotting as described below.

Northern Blot Analysis

The R11C cDNA, which contains the entire rat p50 coding region with 5′ and 3′ untranslated sequences, was EcoRI excised, labeled with α[^{32}P]dCTP by random priming (Boehringer Mannheim Biochemicals), and used to probe a multiple tissue Northern (MTN) blot of adult rat poly(A) RNA (Clontech Laboratories). Hybridization was overnight at

65°C, in Rapid Hyb solution, followed by washes according to the supplier's instructions, except that SSPE was used instead of SSC. Results were detected on a PhosphorImager SF (Molecular Dynamics, Sunnyvale, CA).

Preparation of Tissue Samples

Calf brain and tissue samples from adult male Sprague-Dawley rats (Charles River Laboratories,Wilmington, MA) were homogenized as previously described (Paschal et al., 1992), except that the buffer was 80 mM Pipes, 5 mM EGTA, 1 mM $MgCl_2$, 0.25 M sucrose, 2 mM EDTA, 2 μg/ml leupeptin, 100 μg/ml PMSF, 100 μg/ml TPCK, 2 μg/ml aprotinin, 1 μg/ml pepstatin A. Cytosolic extracts were prepared by centrifugation at 100,000 *g* for 1 h at 4°C. Protein concentrations were determined using the BCA method (Pierce, Rockford, IL). Samples were separated by SDS-PAGE, and either stained with Coomassie blue, or processed for Western blotting as described below.

Cell Culture and Transfections

Cell cultures (Rat2, HeLa, COS-7, and PtK1, all from Amer. Type Culture Collection, Rockville, MD) were maintained as subconfluent monolayers in "growth medium": DMEM (GIBCO/BRL, Life Technologies, Gaithersburg, MD) + 10% FCS (GIBCO/BRL) + 100 U/ml penicillin + 100 μg/ml streptomycin (Sigma Chem. Co., St. Louis, MO). For immunofluorescence staining experiments, cells were trypsinized, and seeded onto sterile 18-mm^2 glass coverslips in six-well dishes (Corning Glass Works, Corning, NY) to reach 70–80% confluency after 48 h.

For transient transfections, cells were seeded onto 18-mm^2 coverslips in six-well dishes at 2–5 × 10^5 cells per well. After 24 h, growth medium was rinsed off with Ca^{++}- and Mg^{++}-free PBS (D-PBS), and replaced with transfection mixture (each well contained 1 μg plasmid DNA with 3.5 μl Lipofectamine reagent (GIBCO/BRL) in 1 ml DMEM, prepared as per supplier's instructions) for 6 h before replacing again with growth medium. Transfected samples destined for biochemical analysis were plated at equivalent densities in 100-mm tissue culture dishes (Corning Glass Works), and treated as above, except that 3 ml of transfection medium was used per dish. Transfected cultures were either fixed or harvested 24–45 h later. Nocodazole (Sigma) was kept as a 1-mg/ml stock in DMSO, and used in all cases at 10 μM for 3–4 h before fixation.

The plasmid used for p50 transfections was made by subcloning the full H50A coding region into the NotI sites of pCMVβ (Clontech), which itself was used as is for β-galactosidase overexpression. The myc epitope tag (MEQKLISEED-stop)(Evan et al., 1985) was inserted after the last p50 codon by PCR mutagenesis and subcloning through a shuttle vector (pARK2mycSTOP, courtesy of Dr. M. A. Gee, Worcester Foundation for Biomedical Research).

Sedimentation Analysis

Cells grown in 100-mm dishes were harvested in D-PBS + 10 mM EDTA, counted, pelleted, and resuspended at equal cell density in buffer "A" (50 mM Tris-Cl [pH 7.5], 150 mM NaCl, 1% NP-40, 1 mM EDTA, 0.5 mM AEBSF, 10 μg/ml leupeptin, 1 mM TAME, 1 μg/ml aprotinin, 1 μg/ml pepstatin A), kept at 4°C for 15 min. Alternatively, pelleted cells were resuspended in buffer A without NP-40 present, and homogenized by two passes at 2,000 rpm in a motor-driven teflon glass homogenizer kept at 4°C. The cell lysates were airfuged at 30 psi for 15 min, and the supernatant (cytosolic extract) was recovered. Sucrose gradients (4.8 ml, 5–20% in buffer A without NP-40) were prepared and 160 μl of each cytosolic extract (corresponding to ~5 × 10^6 cells) was carefully layered on top. These gradients were centrifuged in a SW50.1 rotor (Beckman Instruments, Palo Alto, CA) at 26,500 rpm for 18 h at 4°C, and collected as 350-μl fractions. Sedimentation standards which included alcohol dehydrogenase (5 S), apoferritin (13 S), and thyroglobulin (19 S), were diluted in buffer A, and run with each experiment. Equal volumes of all fractions were analyzed by SDS-PAGE followed by Western blotting, as described above.

Immunological Methods

Antibodies used in this study were "50-1" monoclonal anti-p50 (Paschal et al., 1993), "RA1/10" (Clark and Meyer, 1992) and "A27" affinity-purified rabbit polyclonal anti-Arp1 antisera (gifts from Drs. D. Meyer and S. Clark, UCLA, Los Angeles, CA), "UP235" (for Western blotting) and "UP236" (for immunofluorescence) affinity-purified rabbit polyclonal anti-$p150^{Glued}$ antisera (Waterman-Storer et al., 1995; Melloni et al., 1995) (gifts from Dr. E. Holzbaur, University of Pennsylvania, Philadelphia, PA), "62B" monoclonal anti-p62 (Schafer et al., 1994) (gift from Dr. T. Schroer, Johns Hopkins University, Baltimore, MD), "L5" affinity-purified rabbit polyclonal anti-cytoplasmic dynein intermediate chain (Vaughan and Vallee, 1995), "74.1" monoclonal anti-cytoplasmic dynein intermediate chain (Dillman and Pfister, 1994) (gift from Dr. K. Pfister, University of Virginia, Charlottesville, VA), rabbit antiserum against the myc epitope tag (courtesy of Dr. M.A. Gee, Worcester Foundation for Biomedical Research), "SH" human CREST autoimmune antiserum (Simerly et al., 1990), rabbit polyclonal anti–CENP-E antiserum (Lombillo et al., 1995) ("pAb-1.6", gift from B. Schaar and Dr. T. Yen, Fox Chase Cancer Center, Philadelphia, PA), monoclonal anti-tubulin (DM1A, Amersham), rabbit polyclonal anti-tubulin (gift from Dr. J.C. Bulinski, Columbia University, NY), and monoclonal (Boehringer Mannheim Biochemicals) and rabbit polyclonal (5 Prime - 3 Prime Inc., Boulder, CO) anti–β-galactosidase.

For Western blotting, samples were separated by SDS-PAGE, and electrophoretically transferred to a PVDF membrane (Immobilon P, Millipore, Bedford, MA). After blocking in 5% nonfat dry milk in TBS + 0.1% Tween-20 (TBST) at 4°C overnight, the blot was incubated with primary antibody diluted in TBST + 1% milk for 1 h, washed (3× 10 min in TBST+ 1% milk), and then incubated for 40 min in HRP-conjugated donkey anti–mouse or anti–rabbit IgG diluted 1:10,000 in TBST + 1% milk. After final washing (3× 10 min in TBST), signal detection was achieved by enhanced chemiluminescence (Amersham Corp.).

For immunofluorescence staining, cells grown on glass coverslips were briefly rinsed with D-PBS, and processed according to one of the following protocols. Some samples were preextracted with 1 min incubation in 0.5% Triton X-100 (Pierce, Rockford, IL) in PEMG buffer [80 mM Pipes (pH 6.8), 5 mM EGTA, 1 mM $MgCl_2$, 4 M glycerol], followed by either 10 min in 100% methanol at −20°C, or 15 min in 4% formaldehyde (from 16% EM grade, Electron Microscopy Sciences, Ft. Washington, PA) in PEMG. Some samples ("methanol fixation") were simply incubated for 10 min in 100% methanol at −20°C. Other samples were fixed in 4% formaldehyde in D-PBS for 15 min, followed by either incubation in 0.5% Triton X-100 in D-PBS for 2 min, or 10 min in 100% methanol at −20°C. Samples destined for anti-tubulin staining were simultaneously fixed and extracted ("FGE method") in 4% formaldehyde +0.25% glutaraldehyde (from 8% EM grade, Polysciences Inc., Warrington, PA) +0.5% Triton X-100 in PEMG for 15 min, rinsed in PBS (3 × 5 min), and incubated in 0.5 mg/ml sodium borohydride in PBS (3 × 5 min) to reduce free aldehyde groups.

All samples were then rinsed in PBS (3 × 5 min), incubated in primary antibody solution for 30–45 min, rinsed again in PBS (3 × 5 min), and incubated in secondary antibody solution for 30–40 min. All antibodies were diluted in PBS + 1% normal donkey serum (Jackson Immunoresearch Labs., West Grove, PA). All secondary antibodies were made in donkey, conjugated to DTAF, Texas red, Cy3, or Cy5, and made species-specific by cross-adsorption ("ML" series, Jackson Immunoresearch Labs). Labeling of chromosomal DNA was achieved with a brief incubation in HOECHST dye No. 33258 (Pierce). Samples were mounted in 0.1% *p*-phenylenediamine in PBS + 50% glycerol.

Microscopy Techniques

Conventional immunofluorescence microscopy was carried out on a Zeiss Axiophot photomicroscope (Carl Zeiss Inc., Thornwood, NY) equipped for epifluorescence, and micrographs were taken on Kodak TMAX-400 film. Images were digitized by scanning the negative with a Nikon Coolscan Scanner (Nikon Inc., Electronic Imaging Dept., Melville, NY). Confocal microscopy was carried out on an MRC1000 system (BioRad Microscience, Hercules, CA) equipped with Kr/Ar laser, mounted on a Nikon Diaphot 200 microscope. All digitized images (from conventional and confocal microscopy) were cropped using Adobe Photoshop (version 3.0, Adobe Systems Inc., Mountain View, CA), and imported into Coreldraw (version 5.0, Corel Corp., Ottawa, Canada) for figure assembly. Figures were printed on a Kodak Colorease PS color printer (Eastman Kodak Comp., Rochester, NY).

Results

Molecular Characterization of Mammalian p50

To isolate cDNA clones encoding mammalian p50, amino acid sequences of six tryptic peptides from immunoprecip-

itated calf brain p50 were obtained. One of these (peptide 21, Fig. 1, *a* and *b*) was used to design a mixed oligonucleotide probe (1641I, 38mer) prepared for hybridization screening of a bovine brain cDNA library. This yielded a single 0.4-kb positive clone (B14A) which was found to contain the full peptide 21 sequence (Fig. 1, *a* and *b*). The B14A insert was then used as a hybridization probe to isolate additional p50 clones from a rat brain cDNA library. Of a total of 13 positive clones isolated, two independent rat cDNAs (R11C, R11D) were found to share the same, complete 1,221 bp open reading frame (ORF) encoding 407 residues (Fig. 1 *a*). A homology search of nucleic acid databases also identified a partially characterized human cDNA clone (EST06385, Adams et al., 1993, renamed H50A) which shared extensive identity with B14A. Complete sequencing of clone H50A revealed the same complete ORF found in the rat clones (Fig. 1, *a* and *b*). The deduced full-length rat and human polypeptide sequences are 96% identical (97% similar), and contain all six calf brain p50 tryptic peptide sequences.

The H50A ORF was expressed in bacteria, and the resulting whole cell lysates analyzed by SDS-PAGE and Western blotting using a p50-specific monoclonal antibody (Paschal et al., 1993) (Fig. 2 *a*). A single immunoreactive band in these extracts (lane *2*) was found to migrate slightly above calf brain p50 (lane *1*). We conclude that the ORFs contained in clones H50A, R11C and R11D constitute the full-length coding regions for the 50-kD component of human and rat dynactin complex. We also note the identification of a single p50 chromosomal locus in mouse, thus strongly suggesting the existence of a single p50 gene in mammals (Vaughan, K., A. Mikami, B. Paschal, E. Holzbaur, S. Hughes, C. Echeverri, N. Jenkins, D. Gilbert, K. Moore, N. Copeland, and R. Vallee, manuscript in preparation).

Northern blot analysis of adult rat poly(A)RNA re-

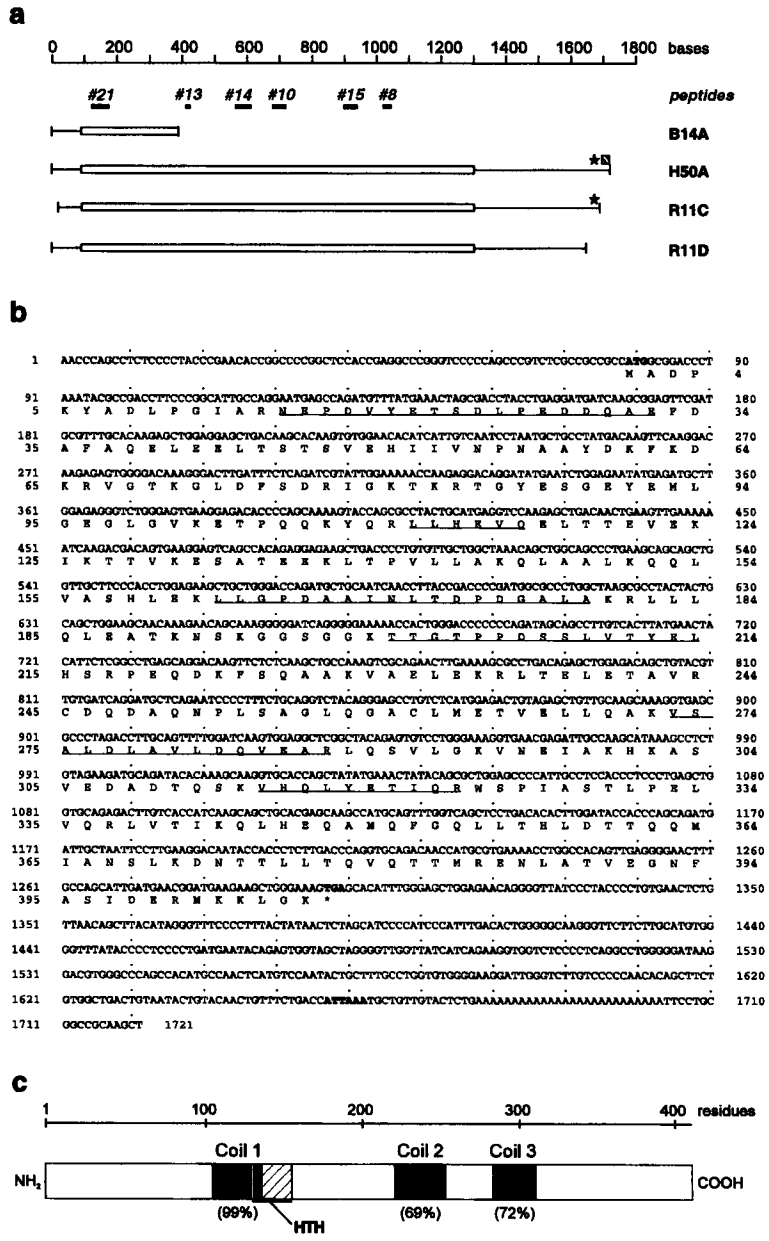

Figure 1. Identification and sequence analysis of mammalian p50-encoding cDNA clones. *(a)* Alignment diagram of bovine (B14A), and full-length human (H50A) and rat (R11C, R11D) p50 cDNA clones, showing relative positions of six calf brain p50 tryptic peptide sequences characterized in this study. The star indicates the position of the hexanucleotide polyadenylation signal sequence (ATTAAA in H50A, and AATAAA in R11C), and the hatched box shows the position of the poly(A) stretch (26mer) in H50A. The open boxes represent the open reading frames (ORF). *(b)* Nucleotide and amino acid sequences of human full-length p50 clone H50A. Note the Kozak consensus box (Kozak, 1991) at the predicted translational initiation site (AUG in bold, at 79), which was preceded by no other inframe methionine codons in this or any other clones characterized in this study. A hexanucleotide polyadenylation signal (ATTAAA in bold, at 1657) and a poly(A) stretch (26mer starting at 1678) are both found downstream from the termination codon (TGA in bold, at 1297). *(c)* Summary diagram of p50 showing probability of predicted coiled-coil domains (in parentheses) and location of prokaryotic HTH motif are shown. Coiled-coil structure was predicted using NEWCOILS (Lupas et al., 1991) with a 28–residue window.

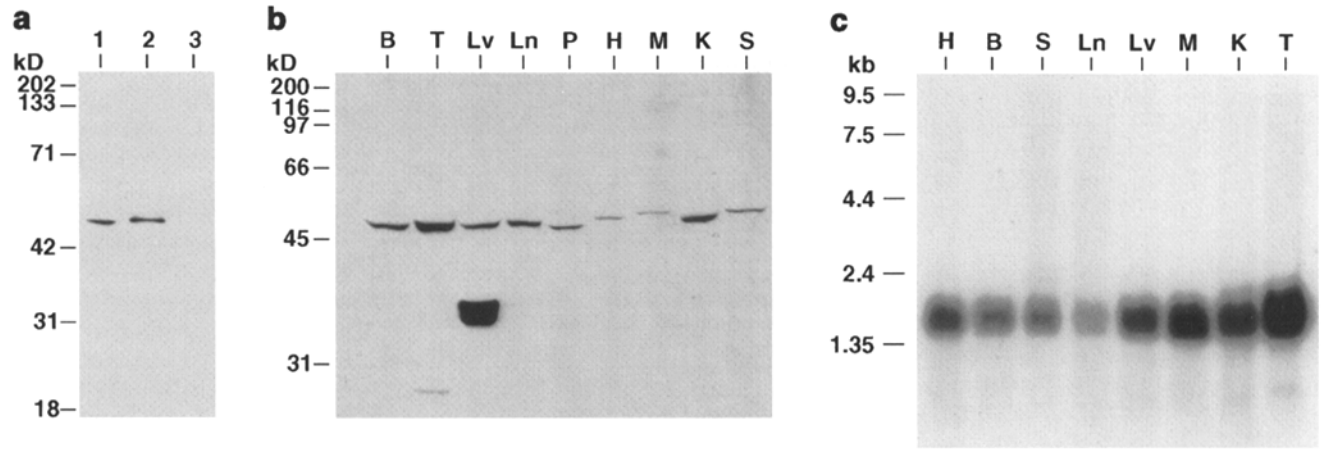

Figure 2. Verification of p50 clone identity and characterization of p50 expression in adult rat tissues. *(a)* Anti-p50 immunoblot (using 50-1 monoclonal antibody) of SDS-PAGE–separated (10% gel) whole cell lysates of *E. coli* strain *BL21(DE3)* transformed with pET14b-driven H50A ORF (lane *2*), compared with calf p50 from brain cytosolic extract (lane *1*) and whole cell lysates from untransformed *BL21(DE3)* culture (lane *3*). The single H50A-encoded protein expressed in bacteria is clearly immunoreactive, and migrates slightly above calf brain p50, but well within the range of variability seen in rat tissues (panel *b*). *(b)* Anti-p50 immunoblots of adult rat tissue cytosolic extracts (25 μg protein/lane) separated by SDS-PAGE (5–18% gradient gel) also reveal a ubiquitous distribution for p50. Variability in electromobility of p50 bands as seen in *a* and *b* was not consistently observed, and is likely due to distortion effects from large bands migrating just above (such as tubulin) or below (such as actin) p50. *(c)* Northern blot of adult rat tissue poly(A) RNA probed with rat full-length p50 clone R11C insert, revealing a single 1.7-kb mRNA species in all tissues tested. Abbreviations: *H*, heart; *B*, brain; *S*, spleen; *Ln*, lung; *Lv*, liver; *M*, skeletal muscle; *K*, kidney, *T*, testis; *P*, pancreas.

vealed a single major 1.7 kb mRNA species in all tissues tested (Fig. 2 *c*). Immunoblotting of adult rat tissue cytosolic extracts (Fig. 2 *b*) also revealed a ubiquitous distribution for p50, consistent with expression patterns observed for other dynactin components (Gill et al., 1991; Clark and Meyer, 1992). The prominent 38-kD doublet detected in liver was not observed in anti-p50 immunoprecipitates (not shown), nor were there any indications of a smaller transcript encoding this species (Fig. 2 *c*).

Rat and human p50 have predicted molecular weights of 44,736 and 44,819 D, respectively, both somewhat lower than the value of 50 kD estimated from SDS-PAGE. The predicted isoelectric points are 4.92 and 4.96, respectively, both consistent with the observed mobility on two-dimensional gel analyses of bovine brain 20 S dynein preparations (Hughes, S.M., and R. Vallee, unpublished observations). Secondary structure predictions indicate an α-helix-rich profile, including three coiled-coil domains, from residues 105 to 135 (99% probability by Newcoils program, Lupas et al., 1991), 219 to 251 (69%), and 281 to 308 (72%) (Fig. 1 *c*). Residues 358 to 404 show a low Newcoils score (19–23%), the significance of which is unclear. A GCG/MOTIF analysis revealed that residues 129 to 154 match the current consensus sequence for the LysR subfamily of helix-turn-helix (HTH) domains (Fig. 1 *c*), indicative of a putative DNA-binding capability. This match, however, was not detected using a BLOCKS analysis (Henikoff and Henikoff, 1991). All members of this HTH subfamily are prokaryotic transcription factors, clearly inconsistent with our current understanding of p50, which has no nuclear localization signal and exhibits no interphase nuclear staining (see below). Nevertheless, this domain may conceivably confer upon p50 a DNA-binding capability which could mediate the kinetochore localization of dynactin during prometaphase (see below).

BLAST and FASTA homology searches using human and rat p50 identified no closely related sequences (other than additional partially characterized human EST clones found to contain p50 sequences). Nevertheless, we note that the predicted structural properties of p50 are comparable to those of the product of the yeast *JNM1* gene, which, like cytoplasmic dynein, is required for proper nuclear migration during mitosis (McMillan and Tatchell, 1994). Jnm1p contains 373 residues, has a predicted molecular weight of 43,620 D, an estimated pI of 4.65, and three predicted coiled-coil domains with sizes and distributions similar to those found in p50 (McMillan and Tatchell, 1994). However, a GCG/BESTFIT comparison of the amino acid sequences shows only 22% identity (47% similarity), spanning the entire sequence (as seen also by GCG/COMPARE and DOTPLOT analyses). Statistical analysis of this comparison using the RDF program (Lipman and Pearson, 1985) yielded a mean score for the optimal p50-Jnm1p alignment of only 4.2 standard deviations (z value) above that of 1,000 randomized sequence sets, indicating this relation to be of negligible significance.

Subcellular Distribution of p50 and Other Dynactin Components

Immunofluorescence microscopy was used to examine the subcellular distribution of p50 in several cultured mammalian cell lines, including HeLa, PtK1, COS-7, and Rat2, all of which yielded equivalent patterns. Fine punctate staining densely filled the entire cytoplasm throughout the cell cycle, and was excluded from the nucleus during interphase (Fig. 3 *a*). Prominent centrosomal staining (Fig. 3, *a* and *b*) was also observed, appearing as a closely spaced group of 2–4 brighter spots (inset in Fig. 3 *a*). These spots were often obscured from late prometaphase to mid-

anaphase by an accumulation of the fine punctate staining along spindle microtubules, particularly toward the spindle poles (Fig. 3 *c, g–k*). Detergent extraction of the cells before fixation abolished most of the fine punctate staining, while the centrosomal spots remained prominent (Fig. 3 *b*). These patterns are consistent with previous reports of anti-Arp1 (Clark and Meyer, 1992), and anti-p150^{Glued} (Gill et al., 1991; Paschal et al., 1993) staining in cultured cells.

Staining of mitotic cells with anti-p50 also showed a strong apparent kinetochore pattern (Fig. 3, *c* and *g*, 4 *a*) beginning after nuclear envelope breakdown (NEB), and disappearing from each chromosome upon its alignment at the metaphase plate (Fig. 3 *c* and *i*). The intensity of the staining was consistent with a time-dependent accumulation of the antigen, from a dim signal just after NEB, to very bright levels in kinetochores of nonaligned metaphase chromosomes (Fig. 3 *c*).

Because kinetochore staining was not observed previously in cells stained with anti-p150^{Glued} antibodies (Gill et al., 1991), we examined the effects of multiple fixation conditions on mitotic staining obtained with a battery of monoclonal and polyclonal antibodies to dynactin components (Table I, Fig. 4). Three independent affinity-purified polyclonal antisera directed against p150^{Glued} (UP236), and Arp1 (RA1/10 and A27) gave kinetochore staining patterns comparable to that seen with the anti-p50 monoclonal antibody (Table I, Fig. 4). Both a monoclonal ("74.1", Table I) and an affinity-purified polyclonal anti-cytoplasmic dynein IC antibody (Vaughan and Vallee, 1995) produced the same kinetochore pattern (Table I, Fig. 4 *e*). Detergent preextraction increased the clarity of kinetochore staining (Table I) apparently by decreasing the fine punctate cytoplasmic staining generally seen with these antibodies (Fig. 3, *a* and *b*). Importantly, all six antibodies also showed clear kinetochore staining in cells fixed without detergent preextraction, thus minimizing the risk of artifactual redistribution of cytosolic antigens (Table I, Fig. 4).

The kinetochore localization of anti-dynactin staining was confirmed by double labeling with a CREST human autoimmune antiserum (Fig. 4, *g–i*). Nocodazole-induced pseudo-prometaphase cells showed enhanced staining of all kinetochores with all anti-dynactin and anti-dynein antibodies. The kinetochores often appeared as paired crescents (Fig. 4 *j*, Figs. 9 and 10) clearly reminiscent of previous electron microscopic observations made under similar microtubule-depolymerizing conditions (Rieder, 1982). We also noted that chromosomes isolated from vinblastine-arrested CHO cells, known to contain little or no tubulin bound to kinetochores (Mitchison and Kirschner, 1985), showed strong anti-p50 staining of the primary constriction (Paschal, B., L. Wordeman, and R. Vallee, unpublished observations).

Cells Overexpressing p50 Show Prometaphase-like Arrest with Aberrant Spindle Morphology

As a first step in investigating p50 and dynactin function in vivo, we transfected COS-7 cells with full-length wild-type and myc-tagged p50. Both constructs produced the same striking phenotypic effects observed throughout the cell cycle. While the present work focuses on the mitotic abnormalities, disruption of the Golgi complex (Echeverri, C.J., and R. Vallee, unpublished observation) and redistribution of endocytic organelles were also noted, and will be described separately (Burkhardt, J., C.J. Echeverri, K.T. Vaughan and R. Vallee, manuscript in preparation).

When analyzed by immunofluorescence microscopy, the overexpressed p50 and p50myc were found diffusely throughout the cytoplasm (Figs. 6 and 7), and were excluded from the nucleus (not shown). A higher than normal proportion of p50- and p50myc-overexpressing cells appeared to be in mitosis, as judged by rounded morphologies and condensed chromosomes. To determine the magnitude of this effect, we compared the cell cycle index of p50myc-overexpressing cells with those of three separate control categories: untransfected cells, transfected but nonexpressing cells, and transfected cells overexpressing an unrelated cytosolic protein, β-galactosidase ("β-gal transfectants") (Fig. 5). From a total of 6,838 p50myc-overexpressing cells counted over four independent experiments, 9.4 ± 1.5% were in M-phase. Nearly all of these (96.3% of mitotic) showed a prometaphase-like chromosome configuration, having clearly undergone chromosome condensation and NEB but not metaphase chromosome alignment (Figs. 6 and 7). Anaphase and telophase configurations were extremely rare in these cells. In striking contrast, the three control categories showed much lower indexes, with 4.2 ± 0.8% of untransfected cells, 4.2 ± 0.6% of transfected nonexpressing cells and 3.6 ± 0.4% of β-gal transfectants found to be distributed throughout M-phase (Fig. 5).

The prometaphase-like p50myc-overexpressing cells were found to show significant spindle aberrations, as revealed by anti-tubulin staining (Figs. 6 and 7). In nearly all cases, two half-spindles were observed, which typically showed marked asymmetry in overall size, shape, and microtubule density, and appeared to be oriented independently. Generally, few or no astral microtubules were visible, and spindle poles were closer than normal to the cell periphery. In most cases, one half-spindle was significantly more developed than the other, as seen in Fig. 6, *d–i*, which shows three clear examples of this phenotype. The microtubules of the larger half-spindle were noticeably longer than those of control mitotic cells, and often formed a loose bundle which curved along the cell periphery as it splayed apart. These elongated microtubules were invariably found to end within the chromosome mass, which often formed a loose, U-shaped configuration around the microtubule bundle (Fig. 6, *e* and *i* and Fig. 7, *a* and *c*).

Triple labeling with anti-p50, anti-tubulin and a human CREST autoimmune anti-centromere antiserum confirmed that all kinetochores of p50myc transfectants colocalized with spindle microtubules (Fig. 7, *c–f*). We also examined the distribution of CENP-E, a kinesin-like protein which accumulates on kinetochores during prometaphase (Yen et al., 1992). Anti–CENP-E staining intensity, which normally shows a marked decrease after metaphase (Yen et al., 1991; Echeverri, C., and R. Vallee, unpublished observations), remained high and revealed kinetochores to be paired in the p50myc-overexpressing cells (Fig. 7 *b*), consistent with the prolongation of a prometaphase-like state.

Tetrapolar spindles were occasionally noted in p50myc

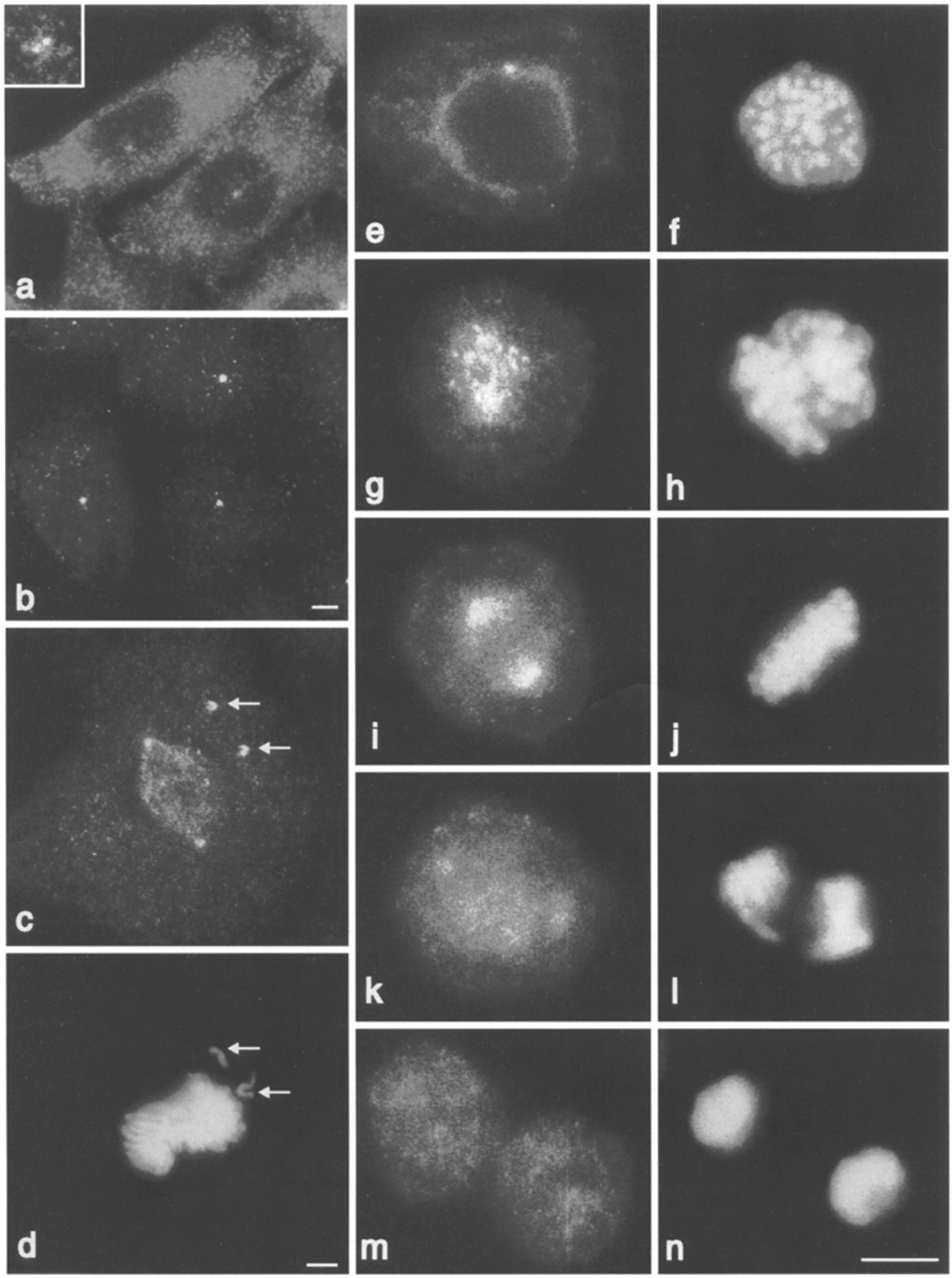

Figure 3. Subcellular distribution of p50 throughout the cell cycle in cultured mammalian cells. *(a, b, c, e, g, i, k,* and *m)* Anti-p50 staining *(d, f, h, j, l,* and *n);* HOECHST DNA staining. (*a* and *b*) Interphase HeLa cells (*c* and *d*); late prometaphase COS-7; (*e* and *f*) prophase Rat2; (*g* and *h*) early prometaphase Rat2; (*i* and *j*) metaphase Rat2; (*k* and *l*) anaphase Rat2; and (*m* and *n*) telophase Rat2. *(a)* Interphase cells fixed in formaldehyde without detergent preextraction show fine punctate staining densely filling the cytoplasm, but excluded from the nucleus. Prominent centrosomal staining is also seen, appearing as 2–4 closely spaced spots at high magnification *(inset). (b)* Cells fixed in formaldehyde after detergent preextraction. Centrosomal staining persists prominently, but most of the fine punctate staining is lost. Centrosomal spots are visible during prophase (*e* and *f*), but become obscured by an accumulation of fine punctate staining along spindle microtubules, particularly near the poles, from prometaphase *(c, d, g,* and *h)* to anaphase *(k* and *l).* Spindle pole staining is often notably dimmer in telophase cells *(m* and *n).* Kinetochore staining was also observed in prometaphase cells *(c, d, g,* and *h)* found most prominent in late-attaching chromosomes before their alignment at the metaphase plate (arrows in *c* and *d).* Cells in *e–n* were fixed in formaldehyde followed by detergent extraction. Kinetochores in panels *c* and *g* would be scored as "+++" and "++", respectively, in Table I. Bars: *a* and *b* shown in *b*; *c* and *d* shown in *d*; for *e–n* shown in *n*, 5 μm.

Table I. Effect of Fixation Methods on Prometaphase Kinetochore Staining with anti-Dynactin and anti-Cytoplasmic Dynein Antibodies in Cultured Vertebrate Cells

	MeOH	Tx-100, then MeOH	Form., then Tx-100	Form., then MeOH	Tx-100, then Form.	Simult. Tx-100, Form. and Glut.
Anti-p50 (mAb "50-1")	+	+++	++	++	+++	−
Anti-p150^{Glued} (pAb "UP236")	++	+++	++	++	+++	nd
Anti-Arpl (pAb "RA1/10")	+	+++	−	++	−	nd
Anti-Arpl (pAb "A27")	++	+++	++	++	+++	±
Anti-IC (pAb "L5")	++	+++	±	±	±	−
Anti-IC (mAb "74.1")	++	+++	±	±	nd	−

+++, prominent staining; ++, clear staining; +, dim staining; ±, variable dim staining; −, no detectable staining; nd, not done. See Materials and Methods for detailed protocols. Abbreviations: *form.*, formaldehyde; *glut.*, glutaraldehyde; *simult.*, simultaneous.

transfectants fixed over 35 h after transfection (as opposed to 27–33 h for most experiments), which were not observed in controls. These cells, which were larger than normal and showed an increased chromosome mass, were probably in their second abnormal mitotic division, having completed the first round without segregating their duplicated pair of centrosomes.

Overexpression of p50 in Cultured Cells Causes Dissociation of the Dynactin Complex

Previous work has shown that in brain and testis cytosolic extracts, p50, p150^{Glued}, and Arp1 all sediment at ~20 S, indicating that they exist exclusively as a complex (Paschal et al., 1993; Clark et al., 1994). To investigate the molecular basis for the cytological defects observed in the present study, cytosolic extracts were prepared from control and transfected cells and analyzed by sucrose density gradient sedimentation (Fig. 8). Extracts of control untransfected and β-gal–transfected COS-7 cultures showed the four dynactin components examined, p150^{Glued}, p62, p50, and Arp1, comigrating at 18 S. This slight divergence from the 20 S value observed previously may reflect tissue-specific differences in dynactin subunit composition, as suggested by p150^{Glued} isoform heterogeneity reported in chicken tissue extracts (Gill et al., 1991). In contrast, all of the dynactin components examined in cultures transfected with either p50myc or untagged p50 (not shown) exhibited the same abnormal behavior. In these samples, p150^{Glued} showed a dramatic shift, exhibiting a major peak at 9 S, and additional streaking throughout the lower end of the gradient. The Arp1 and p62 peaks showed the same small but consistent shift to 16–17 S. Overexpressed myc-tagged and endogenous p50 could be distinguished by a slight difference in electrophoretic mobility. Both species migrated as a single peak at 5 S. The cytoplasmic dynein ICs migrated at 20 S in both control and experimental samples. Identical results were obtained with and without the use of detergent in the cytosol extraction buffer. Thus, these data indicate that dynactin, but not dynein, is specifically disrupted by p50 overexpression.

Cells Overexpressing p50 Show Decreased Dynactin and Cytoplasmic Dynein Staining of Prometaphase Kinetochores

To evaluate the effects of p50myc overexpression on dynactin and cytoplasmic dynein within the cells, mitotic transfectants were examined by immunofluorescence microscopy using antibodies to components of both complexes. Because of the large excess of p50myc in transfected cells, an association of recombinant p50 or p50myc with kinetochores could not be evaluated. However, mitotic transfectants expressing high levels of p50myc showed undetectable or lower than normal kinetochore staining with anti-p150^{Glued} and anti–Arp1 antibodies (not shown). The magnitude of this decrease was found to vary in proportion to the level of p50myc overexpression as judged by immunofluorescence staining intensity. In contrast, kinetochore staining with both anti–CENP-E antiserum (Fig. 7 *b*), and a human CREST anti-centromere auto-antiserum (Fig. 7 *d*) were not affected, arguing that general disruption of kinetochore structure does not occur. Anti-cytoplasmic dynein IC staining of kinetochores, because of its sensitivity to aldehyde fixation (Table I), was difficult to evaluate in these samples.

To maximize the immunofluorescent signal at the kinetochores, and to eliminate potential effects of kinetochore microtubules on antibody accessibility, we examined kinetochore staining in nocodazole-treated cells. As expected, transfected nonexpressing cells and β-gal–transfected cells showed brighter, enlarged kinetochore patterns under these conditions, often appearing crescent shaped (Figs. 9 and 10). In cells overexpressing high levels of p50myc, both anti-Arp1 (Fig. 9 *a*) and anti-p150^{Glued} (Fig. 9 *e*) showed clearly reduced kinetochore staining. Anti-cytoplasmic dynein IC staining of kinetochores in these cells also showed a decrease in intensity (Fig. 10). In general, the morphology of anti-IC–stained kinetochores was more variable than that seen with anti-p150^{Glued} and anti-Arp1, due to the effects of formaldehyde fixation on IC staining. Methanol fixation, which yields optimal kinetochore staining with anti-ICs (Table I), caused excessive

Figure 4. Dynactin and cytoplasmic dynein components localize to kinetochores. Prometaphase COS-7 cells show clear kinetochore staining with anti-p50 (*a*), anti-p150^{Glued} (*c*), anti-Arp1 ("A27") (*g*), and anti-cytoplasmic dynein IC (*e*). *b, d,* and *f* are DNA staining patterns corresponding to *a, c,* and *e*, respectively. Double labeling using anti-Arp1 (*g* and *j*) and human CREST autoimmune serum (*i* and *l*) confirms kinetochore localization of dynactin. The dynactin pattern is restricted to nonaligned kinetochores in control cells (*g–i*), but appears on all kinetochores in nocodazole-treated (10 μm, 3 h at 37°C) cells (*j–l*). *h* and *k* show superimposition of *g* and *i* and *j* and *l*, re-

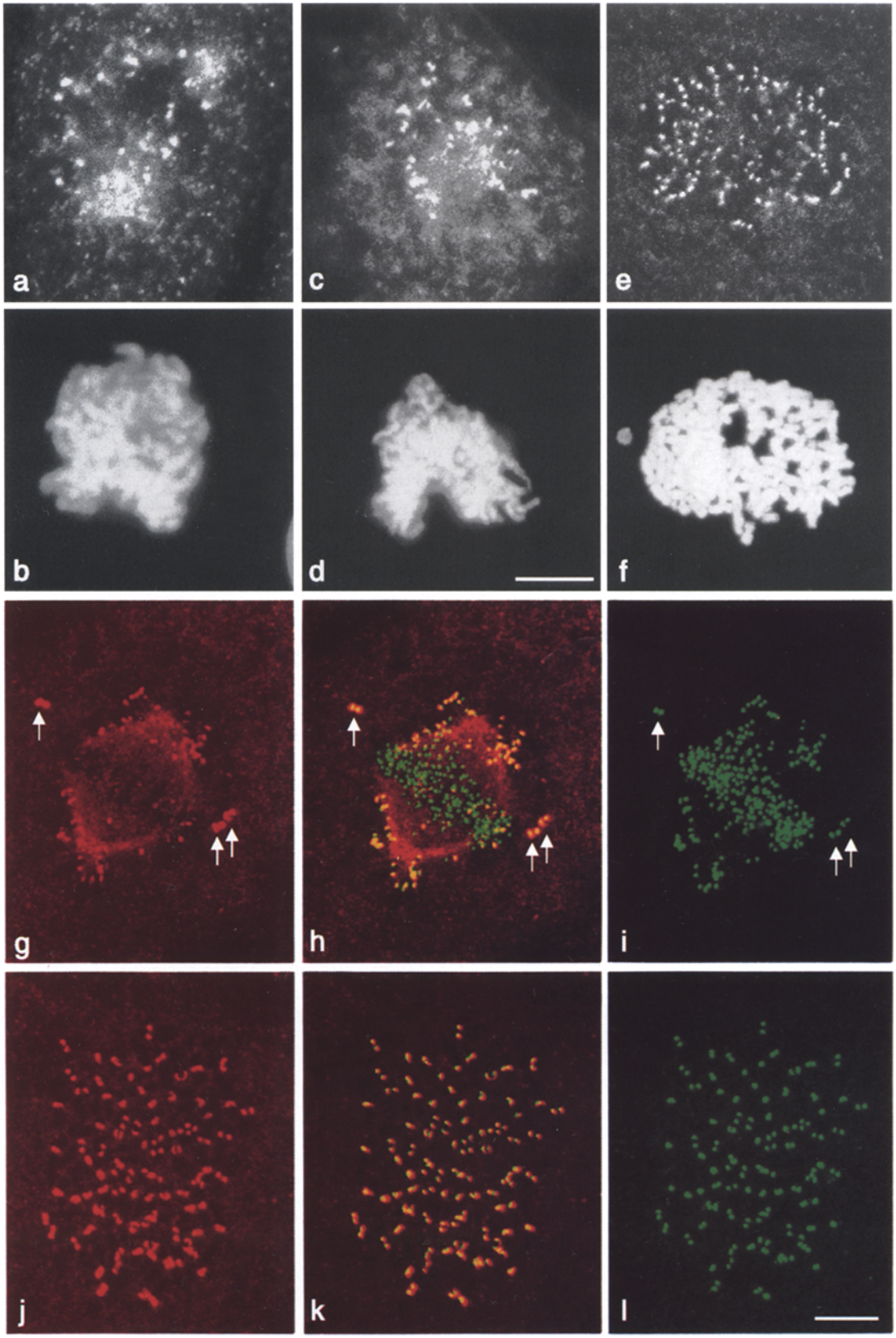

spectively, showing signal colocalization in yellow. *a–f* are conventional fluorescence micrographs, and *g–l* are through-focus maximal projections of complete x/y optical section stacks (22 sections, 0.4 μm step) acquired by confocal microscopy. All cells were fixed in formaldehyde followed by detergent extraction, except *e* and *f* which was fixed directly in methanol. All kinetochores in this figure would be scored as "++" in Table I, except for panel *j* which would be scored "+++". Bars: *a–d* shown in *d*; *e–l* shown in *l*, 10 μm.

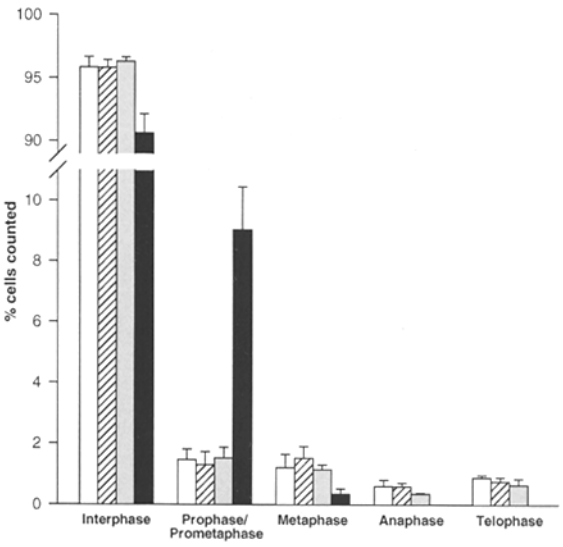

Figure 5. Effect of p50 overexpression on mitotic progression. Cell cycle indexes of control untransfected cells (*open bars*), transfected but nonexpressing cells (*hatched bars*), β-gal transfectants (*shaded bars*), and p50myc transfectants (*black bars*). Cell cycle phases were scored based on chromosome configurations. All values are means from four independent experiments ($507 < n < 3283$ cells/category/experiment) ± SD. Values for p50myc transfectants were found to be significantly different from the three control categories ($p < 0.05$).

loss of mitotic transfected cells, and therefore could not be used in these experiments. Nonetheless, careful examination of numerous p50-overexpressing cells over five separate experiments indicated that the decrease of IC staining at kinetochores was comparable to that seen for anti-Arp1 and anti-p150^{Glued}. In contrast, anti–CENP-E staining at kinetochores remained unchanged under these conditions (Fig. 10 *g*).

Discussion

Subcellular Distribution of Dynactin during Mitosis

That dynactin, like cytoplasmic dynein, associates with prometaphase kinetochores offers clear evidence that the two complexes colocalize within cells, and implicates both in kinetochore function. This conclusion is supported further by our finding that p50 overexpression dramatically disrupts mitosis. Prior reports of the staining patterns obtained with anti-dynein and anti-dynactin antibodies have differed. Cytoplasmic dynein has been found by some laboratories to associate with kinetochores during prometaphase, and subsequently, to appear in a more diffuse pattern toward the spindle poles (Steuer et al., 1990; Pfarr et al., 1990). This pattern has been relatively difficult to see in unextracted cells, and has not been observed universally (Lin and Collins, 1992). Furthermore, a comparable pattern was not observed in cells stained with an antibody against p150^{Glued} (Gill et al., 1991). We report strikingly similar staining for dynactin and cytoplasmic dynein in both detergent preextracted and unextracted cells, and using four different antibodies to three dynactin polypeptides (Arp1, p50, and p150^{Glued}). Anti-IC staining, using two different antibodies, was more sensitive to fixation conditions, perhaps in part reflecting the differences in dynein staining reported among other labs.

As seen for cytoplasmic dynein, we found dynactin immunoreactivity to appear at the kinetochore just after NEB. Staining intensity increased during prometaphase, consistent with the reported maturation of kinetochores during this phase of mitosis (Rieder, 1982), and disappeared upon chromosome alignment at the metaphase plate. We note that the loss of kinetochore staining was delayed in nonattached chromosomes (Fig. 3, *c* and *d* and Fig. 4, *g–i*). This observation indicates that control of dynactin release from kinetochores depends on the specific behavior of individual chromosomes with respect to their interactions with spindle microtubules. While the decrease in kinetochore staining by metaphase could also reflect an antibody accessibility problem, this interpretation is disputed by the multiplicity of independent dynactin and cytoplasmic dynein antibodies which have shown the same pattern in this and previous studies (Pfarr et al., 1990; Steuer et al., 1990). These results are therefore consistent with a role for cytoplasmic dynein and dynactin in kinetochore function before metaphase, but a subsequent role in anaphase cannot be ruled out.

Mitotic Phenotype

Overexpression of p50 resulted in an increase in mitotic index, which correlated with a clear defect in spindle morphology in dividing p50 overexpressors. Based on the range of mitotic index values we observed, we believe that mitosis in the overexpressing cells is prolonged but not completely blocked. Almost all of the mitotic p50-overexpressing cells had achieved centrosome duplication and separation, chromosome condensation, and NEB, but not metaphase chromosome alignment. Kinetochores remained paired, and showed prominent anti–CENP-E staining (Fig. 7). In all of these regards, the cells may be concluded to be in a state comparable to prometaphase. Thus, our observations appear to represent direct in vivo evidence for a role for dynactin, and, therefore, cytoplasmic dynein, in prometaphase. Furthermore, in view of our immunocytochemical observations, these data are also consistent with a direct involvement of both complexes in kinetochore function.

Prometaphase involves a series of events, several of which could conceivably be disrupted by loss of dynactin and cytoplasmic dynein function. After kinetochore maturation (Rieder, 1982), two types of prometaphase chromosome movement have been described, which are, in general, difficult to discriminate temporally but which can be seen as distinct processes in appropriate cells (for review see Rieder and Salmon, 1994). First, in vivo observations of late-attaching chromosomes in newt lung cells revealed the initial capture event to involve a tangential interaction between a kinetochore and the wall of a spindle microtubule (Hayden et al., 1990; Rieder and Alexander, 1990). The monooriented chromosome then exhibited rapid poleward movement along the microtubule at a rate consistent with cytoplasmic dynein-driven organelle motility (Rieder and Alexander, 1990). Interference with dynein motor ac-

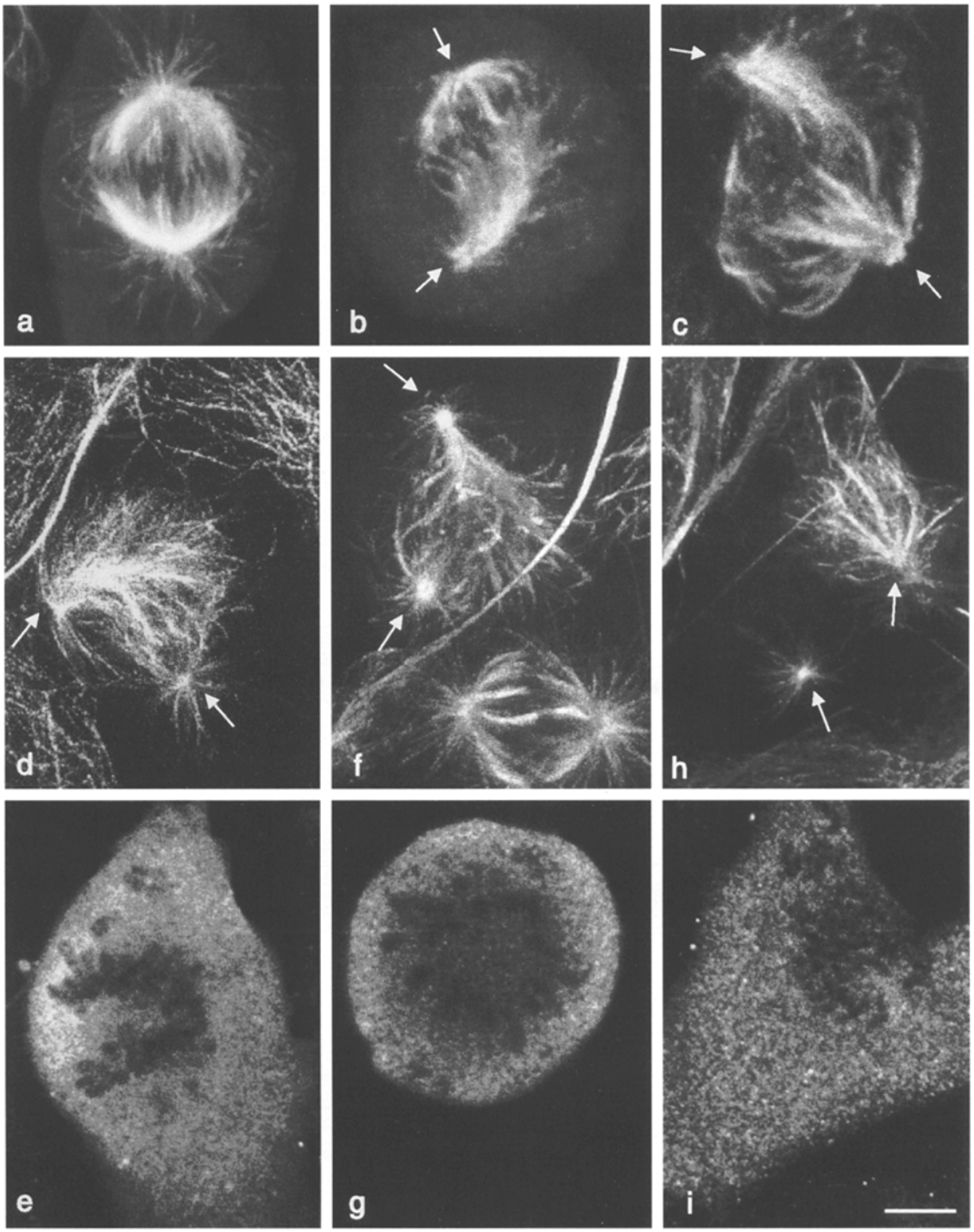

Figure 6. Effects of p50 overexpression on mitotic spindle morphology. Immunofluorescence anti-tubulin staining (*a–d, f* and *h*) of mitotic β-gal–overexpressing COS-7 cell (*a*), and p50myc-overexpressing cells (*b–i*) exhibiting a range of spindle distortions (arrows indicate spindle poles). Panels *b–d, f* and *h* illustrate pronounced asymmetry in microtubule density and orientation of half-spindles, as compared with the unperturbed spindle of a metaphase β-gal–overexpressing COS-7 cell (*a*). Staining of overexpressed p50myc (*e, g,* and *i*) reveals nonrandom chromosome distribution, seen as unstained regions which colocalize with dense areas of distorted spindles (particularly in *e* and *i*). Note nonexpressing mitotic cell in panel *f* as further control. All cells were simultaneously fixed and extracted by "FGE" method (see Materials and Methods). All images were acquired by confocal microscopy. Single optical sections are shown for anti-p50myc staining (*e, g,* and *i*) to facilitate localization of chromosomes. All other panels are through-focus maximal projections of complete x/y optical section stacks (24–40 sections, 0.4 μm step). Bar, 5 μm.

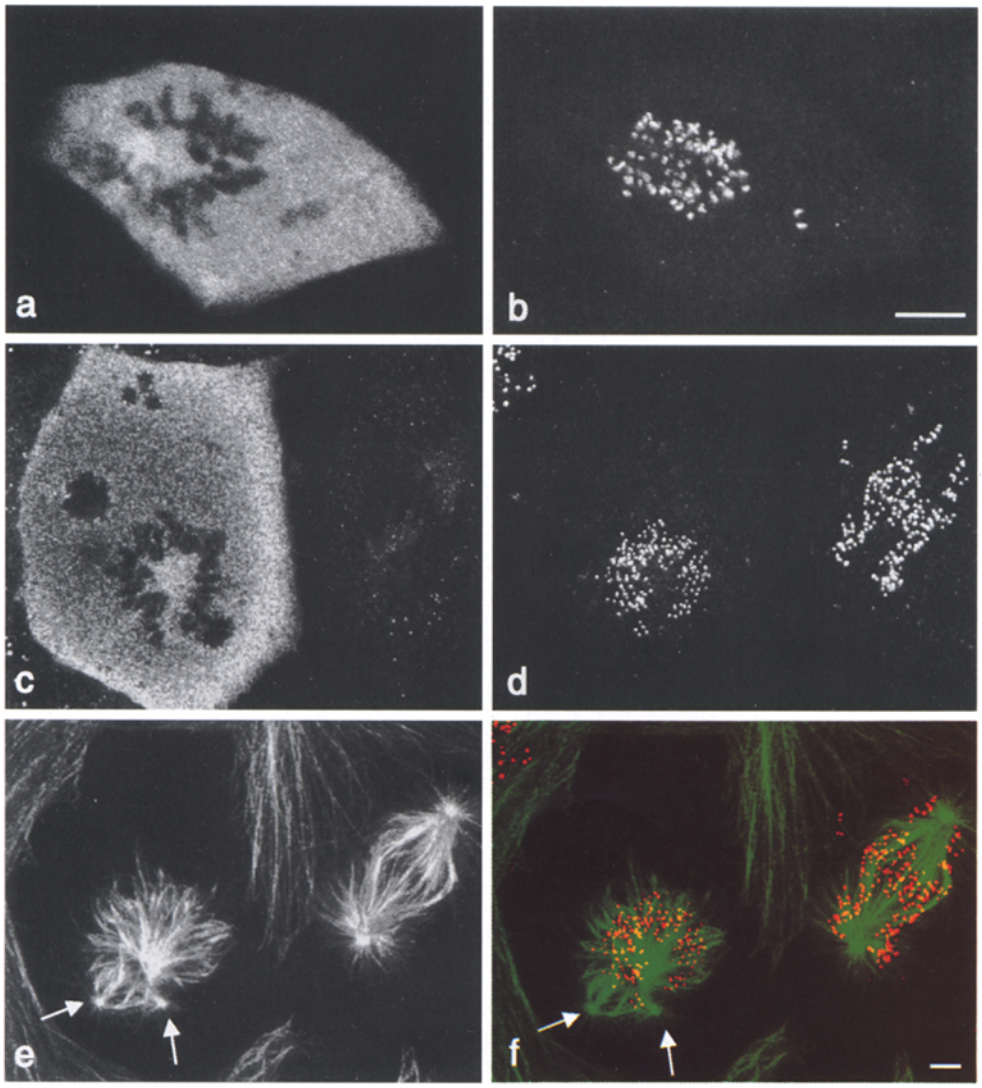

Figure 7. Effect of p50 overexpression on kinetochore proteins. Double immunofluorescence staining of mitotic p50myc-overexpressing cell with anti-p50 (*a*) and anti–CENP-E antiserum (*b*) shows bright staining of paired kinetochores. Triple labeling with anti-p50myc (*c*), human CREST anti-centromere autoimmune serum (*d*), and anti-tubulin (*e*) confirms colocalization of kinetochores with spindle (*f* shows combination of *d* and *e*) (arrows indicate spindle poles). All images were acquired by confocal microscopy. Single optical sections are shown for anti-p50myc staining (*a* and *c*) to facilitate localization of chromosomes. All other panels are through-focus maximal projections of complete x/y optical section stacks (21–22 sections, 0.4 μm step). Cell in *a* and *b* was fixed in formaldehyde followed by methanol, and cell in *c–f* was simultaneously fixed and extracted by "FGE" method (see Materials and Methods). Bars: *a* and *b* shown in *b*; *c–f* shown in *f*, 5 μm.

tivity at this stage would be expected to leave chromosomes at their sites of initial capture, distributed at a variety of distances from the spindle poles. The apparently random distribution of chromosomes along the spindle in p50-overexpressing cells is, therefore, consistent with a role for dynactin and, presumably, dynein in poleward prometaphase movement.

After the initial kinetochore-microtubule interaction, the kinetochore associates with and stabilizes the plus-ends of additional spindle microtubules (Mitchison et al., 1986; Nicklas and Kubai, 1985; Spurck et al., 1990; for a review see Rieder and Salmon, 1994). Chromosome movement is now considerably slower than before and bidirectional, exhibiting low amplitude oscillations (Skibbens et al., 1993), and leading to biorientation and congression to the metaphase plate. Assembly and disassembly of kinetochore microtubules is also intimately coupled to chromosome movement during this and subsequent mitotic phases (Mitchison et al., 1986; Gorbsky et al., 1987; Skibbens et al., 1993; for reviews see Rieder and Salmon, 1994; Desai and Mitchison, 1995). While it is unclear whether or not this type of chromosome movement involves motor activity at all, its onset occurs while both dynein and dynactin are abundant at the kinetochore. Thus, our observation of longer than normal and distorted spindle microtubule bundles in p50-overexpressing cells may also reflect a role for dynactin and dynein during congression, in force production, microtubule dynamics, or both.

The basis for the more general distortion of the mitotic spindle and the displacement of the spindle poles toward the cell periphery in many of the p50-overexpressing cells is uncertain. These effects may be secondary consequences resulting from the loss of kinetochore function. It should be noted, in this regard, that microinjection of CREST anti-centromere antisera, which were found to disrupt kinetochore assembly (Bernat et al., 1991), also result in both chromosome misalignment (Bernat et al., 1990; Simerly et al., 1990), and spindle deformation (Bernat et al., 1990). Alternatively, dynactin and cytoplasmic dynein may have additional cellular sites of action beside the kinetochore, which are responsible for the currently observed effects. Consistent with this possibility, mutational analysis of dynein and dynactin in lower eukaryotes has indicated a role in spindle positioning and elongation, suggesting a primary site of action for the two complexes at the cell cortex (Eshel et al., 1993; Li et al., 1993; Clark and Meyer,

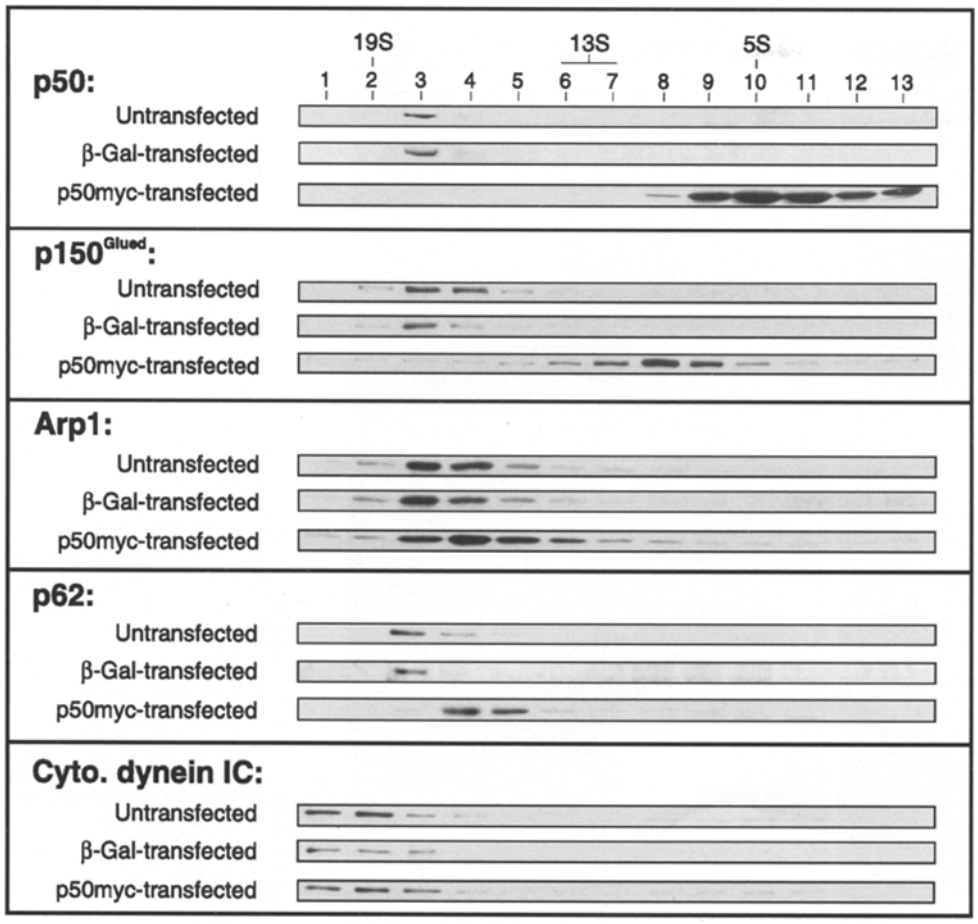

Figure 8. Sedimentation analysis of dynactin and cytoplasmic dynein in p50 overexpressing cultures. Cytosolic extracts of equal numbers of cells from untransfected, β-galactosidase–transfected, and p50myc-transfected COS-7 cultures were subjected to 5–20% sucrose density gradient sedimentation, followed by SDS-PAGE and Western blotting using antibodies to p50, p150^{Glued} ("UP235"), Arp1 ("A27"), p62, and cytoplasmic dynein IC ("74.1"). Peak positions of sedimentation standards are shown.

1994; Muhua et al., 1994; Saunders et al., 1995). Conceivably then, p50 overexpression may effect a comparable role for dynactin and cytoplasmic dynein in vertebrate spindle positioning. In this regard, microinjection of anti-cytoplasmic dynein antibodies into cultured vertebrate cells resulted in a blockage of bipolar spindle formation (Vaisberg et al., 1993), a result which may be consistent with a role for a cortical dynein pool in exerting tension on the spindle poles. We note, however, that the present p50-induced spindle phenotype differs significantly from the phenotype reported in the earlier study, and further work will be needed to reconcile these results.

Molecular Basis for Mitotic Phenotype

The molecular basis for the mitotic phenotype resulting from p50 overexpression appears to be disruption of the dynactin complex. Our sedimentation analysis indicates that p150^{Glued} and p50 detach from the Arp1 filament, which appears to remain intact and maintain its association with p62. This partial dissociation of the dynactin complex may indicate a role for p50 in linking p150^{Glued} to the Arp1 filament. In this view, overexpressed p50 would compete for both p150^{Glued} and Arp1 binding sites. This situation is analogous to that of antigen:antibody excess, in which suprastoichiometric levels of antigen interfere with precipitin formation. Alternatively, the excess p50 may titrate out some limiting structural or regulatory factor critical to the proper assembly of the dynactin complex. Further work will be aimed at discriminating between these models.

The large fraction of dynactin dissociated in the transfected cell extracts indicates that this effect must have occurred at least in part after cell lysis, in view of the heterogeneous nature of the transfected cultures. We estimate that ~10% of the cells in a typical transfected culture overexpress p50 at high level, though lower levels of expression occur in a higher fraction of the cells. Nonetheless, the disruptive effects of p50 appear to be virtually complete in cytosolic extracts. That p50 overexpression disrupts dynactin in the cell as well is strongly supported by our immunocytochemical results, which showed a marked decrease in both p150^{Glued} and Arp1 immunoreactivity at the kinetochore of cells expressing high levels of p50 (Fig. 9). These effects were observed in cells accumulated in mitosis by nocodazole treatment, as well as in non-drug-treated mitotic cells. Nocodazole treatment blocks mitosis before the stage at which dynactin and cytoplasmic dynein normally dissociate from kinetochores (Figs. 4, *j–l* and 9). Even under these conditions, we observed loss of p150^{Glued} and Arp1 kinetochore staining in p50-overexpressing cells. These results support a direct disruption of dynactin by the excess p50, resulting in inhibited recruitment of the complex to prometaphase kinetochores. Why both p150^{Glued} and Arp1 were displaced is uncertain. This observation could either mean that p50 is important in tar-

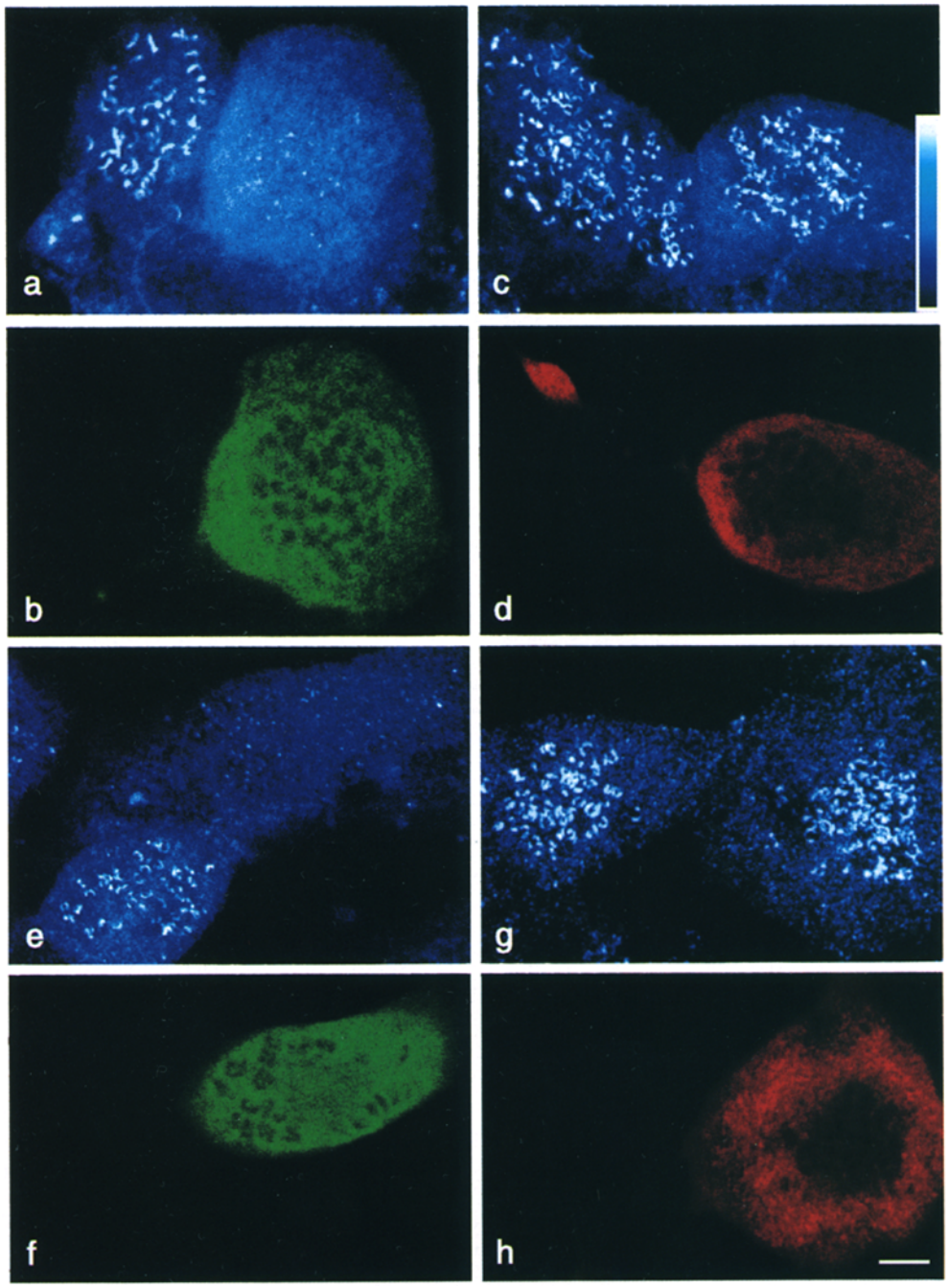

Figure 9. Effect of p50 overexpression on anti-Arp1 and anti-p150^{Glued} staining of kinetochores. Nocodazole-treated (10 μm, 3 h at 37°C) COS-7 cells transfected with p50myc (*a, b, e,* and *f*), or β-galactosidase (*c, d, g,* and *h*) were stained with "A27" anti-Arp1 (*a* and *c*) or anti-p150^{Glued} (*e* and *g*). Anti-p50myc (*b* and *f*) and anti–β-galactosidase (*d* and *h*) staining identifies overexpressing cells, and reveals chromosomal localization as unstained regions. Neighboring nonexpressing prometaphase cells offer an internal control in each field of view, to assess the decrease in anti-Arp1 and anti-p150^{Glued} kinetochore staining intensity. *a, c, e,* and *g* are through-focus maximal projections of complete x/y optical section stacks (14–22 sections, 0.35 μm step). *b, d, f,* and *h* are single optical sections to facilitate visualization of chromosomes in overexpressing cells. Anti-Arp1 and anti-p150^{Glued} staining are displayed in pseudocolor to show intensity differences (color range shown in panel *c*). All cells were fixed in formaldehyde followed by methanol extraction. Bar, 5 μm.

geting dynactin to the kinetochore, or that the complex becomes relatively unstable after p50-induced dissociation.

In view of the distinctive disruptive effects of p50 overexpression on both the dynactin complex and mitotic progression, we propose the name dynamitin for this polypeptide.

Role of Dynactin in Cytoplasmic Dynein Function

In addition to its effect on other components of the dynactin complex, dynamitin/p50 overexpression caused a clear decrease in the association of cytoplasmic dynein with the kinetochore. This result implies a role for dynactin in mediating the association of cytoplasmic dynein with kinetochores and other organelles. Two general models for dynactin function may be envisaged. First, it may serve to regulate dynein activity. Dynactin was, in fact, initially described on the basis of its effect in stimulating the frequency of dynein-mediated organelle movements along microtubules in vitro (Gill et al., 1991; Schroer and Sheetz, 1991). Alternatively, dynactin may serve to mediate the binding of dynein to subcellular structures destined for retrograde transport. According to this model, inactivation of dynactin should serve to dissociate dynein from its subcellular binding sites, and this is, in fact, what we observe. This latter model is also strongly supported by our recent identification of p150^{Glued} as an IC-binding protein, especially in light of the role of the axonemal dynein ICs in

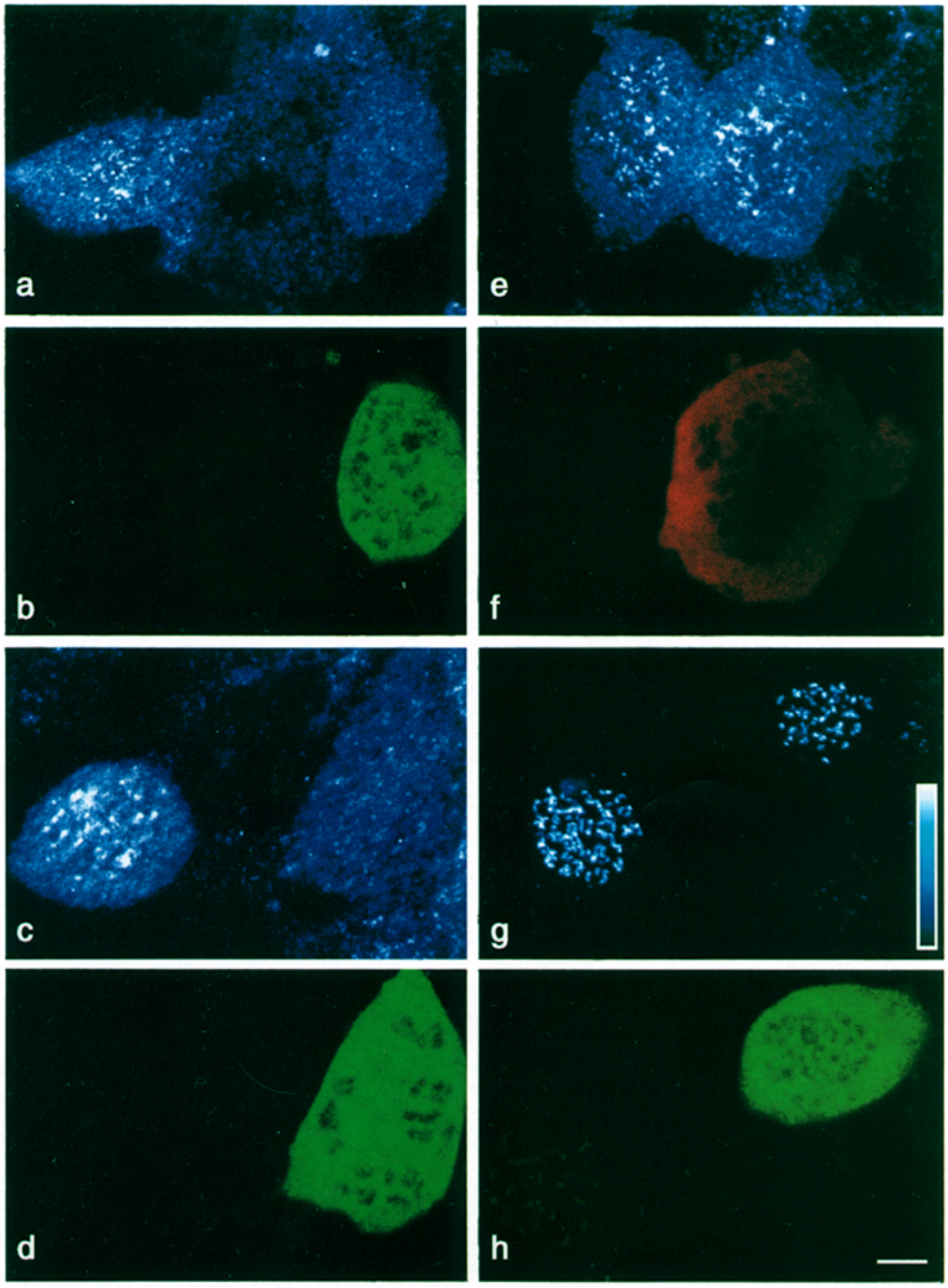

Figure 10. Effect of p50 overexpression on anti-cytoplasmic dynein and anti–CENP-E staining of kinetochores. Nocodazole-treated (10 μm, 3 h at 37°C) COS-7 cells transfected with p50myc (*a–d, g* and *h*), or β-galactosidase (*e* and *f*) were stained with anti-cytoplasmic dynein IC (*a, c,* and *e*), or anti–CENP-E antiserum (*g*). Anti-p50myc (*b, d,* and *h*) and anti–β-galactosidase (*f*) staining identifies overexpressing cells, and reveals chromosomal localization as unstained regions. Neighboring nonexpressing prometaphase cells offer an internal control in panels *a, c, e,* and *g* to assess the differences in kinetochore staining intensity. *a, c, e,* and *g* are through-focus maximal projections of complete x/y optical section stacks (20–26 sections, 0.4 μm step). *b, d, f,* and *h* are single optical sections to facilitate visualization of chromosomes in overexpressing cells. Anti-IC and anti–CENP-E staining are displayed in pseudocolor to show intensity differences (color range shown in panel *g*). All cells were fixed in formaldehyde followed by methanol extraction. Bar, 5 μm.

targeting to the flagellar outer doublet microtubules (King and Witman, 1990; Paschal et al., 1992; Vaughan and Vallee, 1995; Karki and Holzbaur, 1995).

Dynactin may, therefore, serve as a "receptor" for cytoplasmic dynein on the surface of membranous organelles and kinetochores. However, it is structurally distinct from known cell surface receptors and its mode of attachment to kinetochores and membranous organelles is unknown. It is also likely to serve as more than an anchor for cytoplasmic dynein, especially with regard to kinetochore function. The p150^{Glued} subunit of dynactin has been found to contain a microtubule-binding domain (Pierre et al., 1992; Waterman-Storer et al., 1995). This domain could conceivably participate in kinetochore capture by mitotic microtubules. However, activity of this domain must be regulated if force production by cytoplasmic dynein is to result in productive poleward chromosome movement. Conceivably, the domain is active transiently, to serve in loading kinetochores onto the kinetochore-to-pole microtubules. This process itself could be complex, involving a sequential tangential and end-on attachment of kinetochores to microtubules. Alternatively, it is possible that dynactin is required throughout the transport process and that its microtubule-binding activity is regulated coordinately with the dynein cross-bridge cycle. Resolution of these issues promises to provide further insight into the mechanism of mitosis and of organelle movement.

The authors would like to thank Dr. Erika Holzbaur for the gift of anti-p150^{Glued} antibodies, Drs. David Meyer and Sean Clark for anti-Arp1 anti-

bodies, Dr. Trina Schroer for monoclonal anti-p62, Dr. Kevin Pfister for anti-IC, Dr. Tim Yen and Bruce Schaar for anti–CENP-E antiserum, Dr. B. Brinkley for the CREST antiserum, Dr. J.-C. Bulinski for anti-tubulin antiserum, and Dr. M. Gee for rabbit anti-myc antiserum. Many thanks also go out to Dr. John Leszyk of the Worcester Foundation for Biomedical Research Protein Chemistry Facility for performing the HPLC and microsequencing, and to Sharon Hughes, Kip Sluder, Beth Luna, and Curt Wilkerson for many helpful discussions.

This work was supported by National Institutes of Health (NIH) grants GM43474 to R.B. Vallee and GM15941 to K.T. Vaughan, and a Natural Sciences and Engineering Research Council (Canada) predoctoral scholarship to C.J. Echeverri.

Received for publication 28 July 1995 and in revised form 7 November 1995.

References

Adams, M.D., M. Bento Soares, A.R. Kerlavage, C. Fields, and J.C. Venter. 1993. Rapid cDNA sequencing (expressed sequence tags) from a directionally cloned human infant brain cDNA library. *Nature Genet.* 4:373–380.

Aebersold, R. 1989. *In* A Practical Guide to Protein and Peptide Purification for Microsequencing. P.R. Matsudaira, editor. Academic Press, San Diego, CA. 71–88.

Altschul, S.F., W. Gish, W. Miller, E.W. Myers, and D.J. Lipman. 1990. Basic local alignment search tool. *J. Mol. Biol.* 215:403–410.

Aniento, F., N. Emans, G. Griffiths, and J. Gruenberg. 1993. Cytoplasmic dynein-dependent vesicular transport from early to late endosomes. *J. Cell Biol.* 123:1373–1387.

Bernat, R.L., G.G. Borisy, N.F. Rothfield, and W.C. Earnshaw. 1990. Injection of anticentromere antibodies in interphase disrupts events required for chromosome movement at mitosis. *J. Cell Biol.* 111:1519–1533.

Bernat, R.L., M.R. Delannoy, N.F. Rothfield, and W.C. Earnshaw. 1991. Disruption of centromere assembly during interphase inhibits kinetochore morphogenesis and function in mitosis. *Cell.* 66:1229–1238.

Clark, S.W., and D.I. Meyer. 1992. Centractin is an actin homologue associated with the centrosome. *Nature (Lond.).* 359:246–250.

Clark, S.W., and D.I. Meyer. 1994. *ACT3*: a putative centractin homologue in *S. cerevisiae* is required for proper orientation of the mitotic spindle. *J. Cell Biol.* 127:129–138.

Clark, S.W., O. Staub, I.R. Clark, E.L. F. Holzbaur, B.M. Paschal, R.B. Vallee, and D.I. Meyer. 1994. β-Centractin: characterization and distribution of a new member of the centractin family of actin-related proteins. *Mol. Biol. Cell.* 5:1301–1310.

Collins, C.A., and R.B. Vallee. 1989. Preparation of microtubules from rat liver and testes:cytoplasmic dynein is a major microtubule-associated protein. *Cell Motil. Cytoskeleton.* 14:491–500.

Corthésy-Theulaz, I., A. Pauloin, and S.R. Pfeffer. 1992. Cytoplasmic dynein participates in the centrosomal localization of the Golgi complex. *J. Cell Biol.* 118:1333–1345.

Desai, A., and T.J. Mitchison. 1995. A new role for motor proteins as couplers to depolymerizing microtubules. *J. Cell Biol.* 128:1–4.

Dillman, J.F., and K.K. Pfister. 1994. Differential phosphorylation in vivo of cytoplasmic dynein associated with anterogradely moving organelles. *J. Cell Biol.* 127:1671–1681.

Eshel, D., L.A. Urrestarauzu, S. Vissers, J.C. Jauniaux, J.C. van Vliet-Reedijk, R.J. Planta, and I.R. Gibbons. 1993. Cytoplasmic dynein is required for normal nuclear segregation in yeast. *Proc. Natl. Acad. Sci. USA.* 90:11172–11176.

Evan, G.I., G.K. Lewis, G. Ramsay, and J.M. Bishop. 1985. Isolation of monoclonal antibodies specific for human *c-myc* proto-oncogene product. *Mol. Cell. Biol.* 5:3610–3616.

Fath, K.R., G.M. Trimbur, and D.R. Burgess. 1994. Molecular motors are differentially distributed on Golgi membranes from polarized epithelial cells. *J. Cell Biol.* 126:661–675.

Gill, S.R.T., T.A. Schroer, I. Szilak, E.R. Steuer, M.P. Sheetz, and D.W. Cleveland. 1991. Dynactin, a conserved, ubiquitously expressed component of an activator of vesicle motility mediated by cytoplasmic dynein. *J. Cell Biol.* 115:1639–1650.

Gorbsky, G.J., P.J. Sammak, and G.G. Borisy. 1987. Chromosomes move poleward in anaphase along stationary microtubules that coordinately disassemble from their kinetochore ends. *J. Cell Biol.* 104:9–18.

Harte, P.J., and D.R. Kankel. 1982. Genetic analysis of mutations at the *Glued* locus and interacting loci in *Drosophila melanogaster*. *Genetics.* 101:477–501.

Hayden, J.H., S.S. Bowser, and C.L. Rieder. 1990. Kinetochores capture astral microtubules during chromosome attachment to the mitotic spindle: direct visualization in live newt lung cells. *J. Cell Biol.* 111:1039–1045.

Henikoff, S., and J.G. Henikoff. 1994. Protein family classification based on searching a database of blocks. *Genomics.* 19:97–107.

Holzbaur, E.L.F., J.A. Hammarback, B.M. Paschal, N.G. Kravit, K.K. Pfister, and R.B. Vallee. 1991. Homology of a 150 kD cytoplasmic dynein-associated polypeptide with the *Drosophila* gene *Glued*. *Nature (Lond.).* 351:579–583.

Holzbaur, E.L.F., and R.B. Vallee. 1994. Dyneins: molecular structure and cellular function. *Annu. Rev. Cell Biol.* 10:339–372.

Hyman, A.A., and T.J. Mitchison. 1991. Two different microtubule-based motor activities with opposite polarities in kinetochores. *Nature (Lond.).* 351: 206–211.

Jacobs, K.A., R. Rudersdorf, S.D. Neill, J.P. Dougherty, E.L. Brown, and E.F. Fritsch. 1988. The thermal stability of oligonucleotide duplexes is sequence independent in tetraalkylammonium salt solutions: application to identifying recombinant DNA clones. *Nucleic Acids Res.* 16:4637–4650.

Karki, S., and E.L.F. Holzbaur. 1995. Affinity chromatography demonstrates a direct binding between cytoplasmic dynein and the dynactin complex. *J. Biol. Chem.* 270:28806–28811.

King, S.M., and G.B. Witman. 1990. Localization of an intermediate chain of outer arm dynein by immunoelectron microscopy. *J. Biol. Chem.* 265:19807–19811.

Kozak, M. 1991. An analysis of vertebrate mRNA sequences: intimations of translational control. *J. Cell Biol.* 115:887–903.

Lacey, M.L., and L.T. Haimo. 1992. Cytoplasmic dynein is a vesicle protein. *J. Biol. Chem.* 267:4793–4798.

Lees-Miller, J.P., D.M. Helfman, and T.A. Schroer. 1992. A vertebrate actin-related protein is a component of a multi-subunit complex involved in microtubule-based vesicle motility. *Nature (Lond.).* 359:244–246.

Li, Y.Y., E. Yeh, T. Hays, and K. Bloom. 1993. Disruption of mitotic spindle orientation in a yeast dynein mutant. *Proc. Natl. Acad. Sci. USA.* 90:10096–100100.

Lin, S.X., and C.A. Collins. 1992. Immunolocalization of cytoplasmic dynein to lysosomes in culture cells. *J. Cell Sci.* 101:125–137.

Lipman, D.J., and W.R. Pearson. 1985. Rapid and sensitive protein similarity searches. *Science (Wash. DC).* 227: 1435–1441.

Lipman, D.J., and W.R. Pearson. 1988. Improved tools for biological sequence comparison. *Proc. Natl. Acad. Sci. USA.* 85:2444–2448.

Lombillo, V.A., C. Nislow, T.J. Yen, V.I. Gelfand, and J.R. McIntosh. 1995. Antibodies to the kinesin motor domain and CENP-E inhibit microtubule depolymerization-dependent motion of chromosomes in vitro. *J. Cell Biol.* 128:107–115.

Lupas, A., M. Van Dyke, and J. Stock. 1991. Predicting coiled coils from protein sequences. *Science (Wash. DC).* 252:1162–1164.

McGrail, M., J. Gepner, A. Silvanovich, S. Ludmann, M. Serr, and T.S. Hays. 1995. Regulation of cytoplasmic dynein function in vivo by the *Drosophila Glued* complex. *J. Cell Biol.* 131:411–425.

McMillan, J.N., and K. Tatchell. 1994. The *JNM1* gene in the yeast *Saccharomyces cerevisiae* is required for nuclear migration and spindle orientation during the mitotic cell cycle. *J. Cell Biol.* 125:143–158.

Melloni, R.H., Jr., M.K. Tokito, and E.L.F. Holzbaur. 1995. Expression of the $p150^{Glued}$ component of the dynactin complex in developing and adult rat brain. *J. Comp. Neurol.* 357:15–24.

Mitchison, T.J., and M.W. Kirschner. 1985. Properties of the kinetochore in vitro. I. Microtubule nucleation and tubulin binding. *J. Cell Biol.* 101:755–765.

Mitchison, T.J., L. Evans, E. Schultz, and M.W. Kirschner. 1986. Sites of microtubule assembly and disassembly in the mitotic spindle. *Cell.* 45:515–527.

Muhua, L., T.S. Karpova, and J.A. Cooper. 1994. A yeast actin-related protein homologous to that found in vertebrate dynactin complex is important for spindle orientation and nuclear migration. *Cell.* 78:669–679.

Nicklas, R.B., and D.F. Kubai. 1985. Microtubules, chromosome movement, and reorientation after chromosomes are detached from the spindle by micromanipulation. *Chromosoma.* 92:313–324.

Paschal, B.M., and R.B. Vallee. 1987. Retrograde transport by the microtubule associated protein MAP 1C. *Nature (Lond.).* 330:181–183.

Paschal, B.M., A. Mikami, K.K. Pfister, and R.B. Vallee. 1992. Homology of the 74-kD cytoplasmic dynein subunit with a flagellar dynein polypeptide suggests an intracellular targeting function. *J. Cell Biol.* 118:1133–1143.

Paschal, B.M., E.L.F. Holzbaur, K.K. Pfister, S. Clark, D.I. Meyer, and R.B. Vallee. 1993. Characterization of a 50 kD polypeptide in cytoplasmic dynein preparations reveals a complex with $p150^{Glued}$ and a novel actin. *J. Biol. Chem.* 268:15318–15323.

Pfarr, C.M., M. Coue, P.M. Grisson, T.S. Hays, M.E. Porter, and J.R. McIntosh. 1990. Cytoplasmic dynein is localized to kinetochores during mitosis. *Nature (Lond.).* 345:263–265.

Pierre, P., J. Scheel, J.E. Rickard, and T.E. Kreis. 1992. CLIP-170 links endocytic vesicles to microtubules. *Cell.* 70:887–900.

Plamann, M., P.F. Minke, J.H. Tinsley, and K.S. Bruno. 1994. Cytoplasmic dynein and actin-related protein Arp-1 are required for normal nuclear distribution in filamentous fungi. *J. Cell Biol.* 127:139–149.

Rieder, C.L. 1982. The formation, structure, and composition of the mammalian kinetochore and kinetochore fiber. *Int. Rev. Cytol.* 79:1–58.

Rieder, C.L., and S.P. Alexander. 1990. Kinetochores are transported poleward along a single astral microtubule during chromosome attachment to the spindle in newt lung cells. *J. Cell Biol.* 110:81–95.

Rieder, C.L., and E.D. Salmon. 1994. Motile kinetochores and polar ejection forces dictate chromosome position on the vertebrate mitotic spindle. *J. Cell Biol.* 124:223–233.

Saunders, W.S., D. Koshland, D. Eshel, I.R. Gibbons, and M.A. Hoyt. 1995. *Saccharomyces cerevisiae* kinesin- and dynein-related proteins required for

anaphase chromosome segregation. *J. Cell Biol.* 128:617–624.
Schafer, D.A., S.R. Gill, J.A. Cooper, J.E. Heuser, and T.A. Schroer. 1994. Ultrastructural analysis of the dynactin complex: an actin-related protein is a component of a filament that resembles F-actin. *J. Cell Biol.* 126:403–412.
Schnapp, B.J., and T.S. Reese. 1989. Dynein is the motor for retrograde axonal transport of organelles. *Proc. Natl. Acad. Sci. USA.* 86:1548–1552.
Schroer, T.A., and M.P. Sheetz. 1991. Two activators of microtubule-based vesicle transport. *J. Cell Biol.* 115:1309–1318.
Schroer, T.A., E.R. Steuer, and M.P. Sheetz. 1989. Cytoplasmic dynein is a minus end-directed motor for membranous organelles. *Cell.* 56:937–946.
Simerly, C., R. Balczon, B.R. Brinkley, and G. Schatten. 1990. Microinjected kinetochore antibodies interfere with chromosome movement in meiotic and mitotic mouse oocytes. *J. Cell Biol.* 111:1491–1504.
Skibbens, R.V., V.P. Skeen, and E.D. Salmon. 1993. Directional instability of kinetochore motility during chromosome congression and segregation in mitotic newt lung cells: a push-pull mechanism. *J. Cell Biol.* 122:859–875.
Spurck, T.P., O.G. Stonington, J.A. Snyder, J.D. Pickett-Heaps, A. Bajer, and J. Mole-Bajer. 1990. UV microbeam irradiations of the mitotic spindle. II. Spindle fiber dynamics and force production. *J. Cell Biol.* 111:1505–1518.
Steuer, E.R., L. Wordeman, T.A. Schroer, and M.P. Sheetz. 1990. Localization of cytoplasmic dynein to mitotic spindles kinetochores. *Nature (Lond.).* 345: 266–268.
Vaisberg, E.A., M.P. Koonce, and J.R. McIntosh. 1993. Cytoplasmic dynein plays a role in mammalian mitotic spindle formation. *J. Cell Biol.* 123:849–858.
Vaughan, K.T., and R.B. Vallee. 1995. Cytoplasmic dynein binds dynactin through a direct interaction between the intermediate chains and $p150^{Glued}$. *J. Cell Biol.* 131:1507–1516.
Waterman-Storer, C.M., S. Karki, and E.L.F. Holzbaur. 1995. The $p150^{Glued}$ component of the dynactin complex binds to both microtubules and the actin-related protein centractin (Arp-1). *Proc. Natl. Acad. Sci. USA.* 92:1634–1638.
Xiang, X., S.M. Beckwith, and N.R. Morris. 1994. Cytoplasmic dynein is involved in nuclear migration in *Aspergillus nidulans*. *Proc. Natl. Acad. Sci. USA.* 91:2100–2104.
Yen, T.J., D.A. Compton, D. Wise, R.P. Zinkowski, B.R. Brinkley, W.C. Earnshaw, and D.W. Cleveland. 1991. CENP-E, a novel centromere associated protein required for progression from metaphase to anaphase. *EMBO (Eur. Mol. Biol. Organ.) J.* 10:1245–1254.
Yen, T.J., G. Li, B.T. Schaar, I. Szilak, and D.W. Cleveland. 1992. CENP-E is a putative kinetochore motor that accumulates just before mitosis. *Nature (Lond.).* 359:536–539.